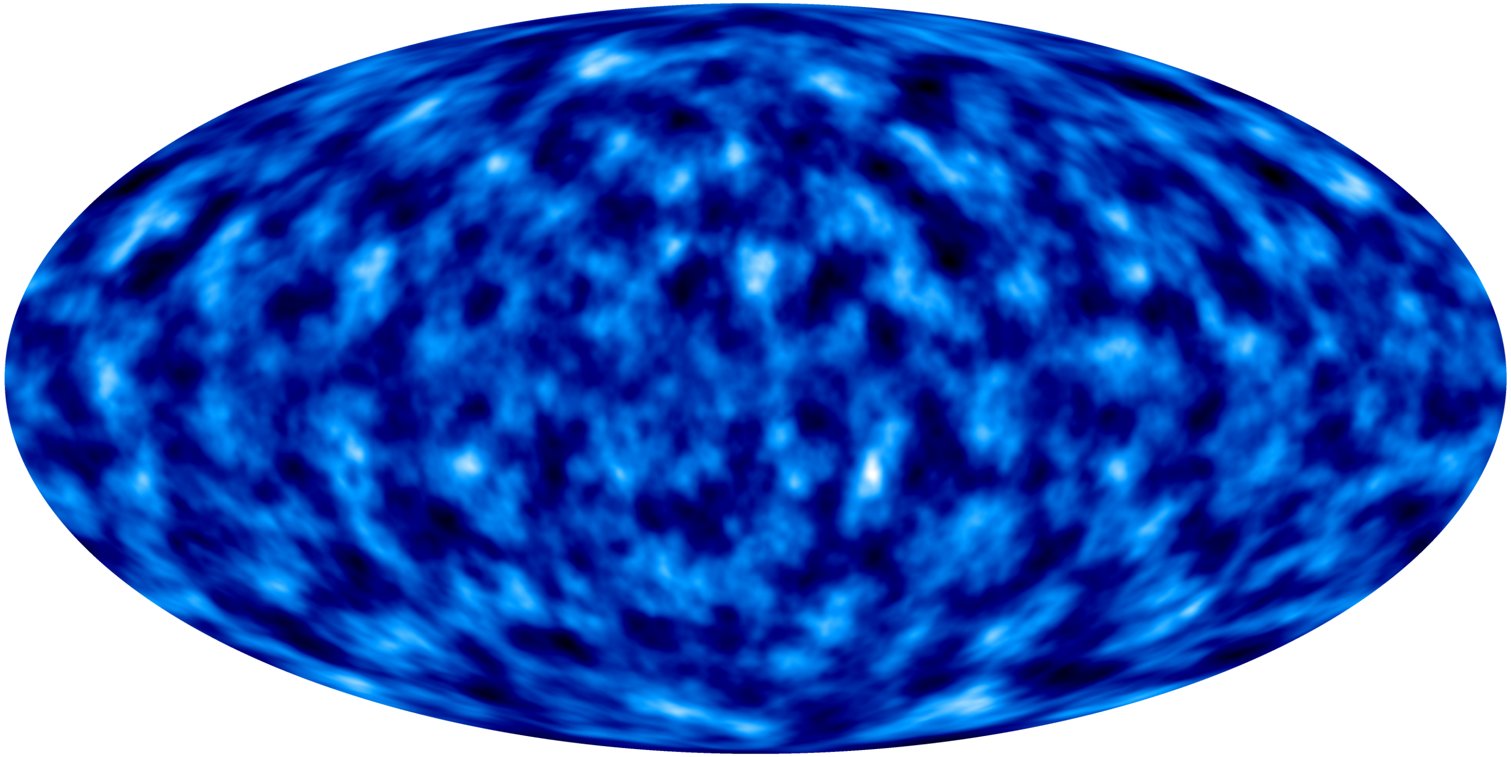

CMB lensing results from PLANCK

Laurence Perotto, LPSC/CNRS on behalf of the Planck Collaboration

planck esa HFi PLANCK PLANCK LFI

CMB lensing from Planck

mostly based on 2 Planck papers:

***Planck* 2015 results. XV. Gravitational lensing**

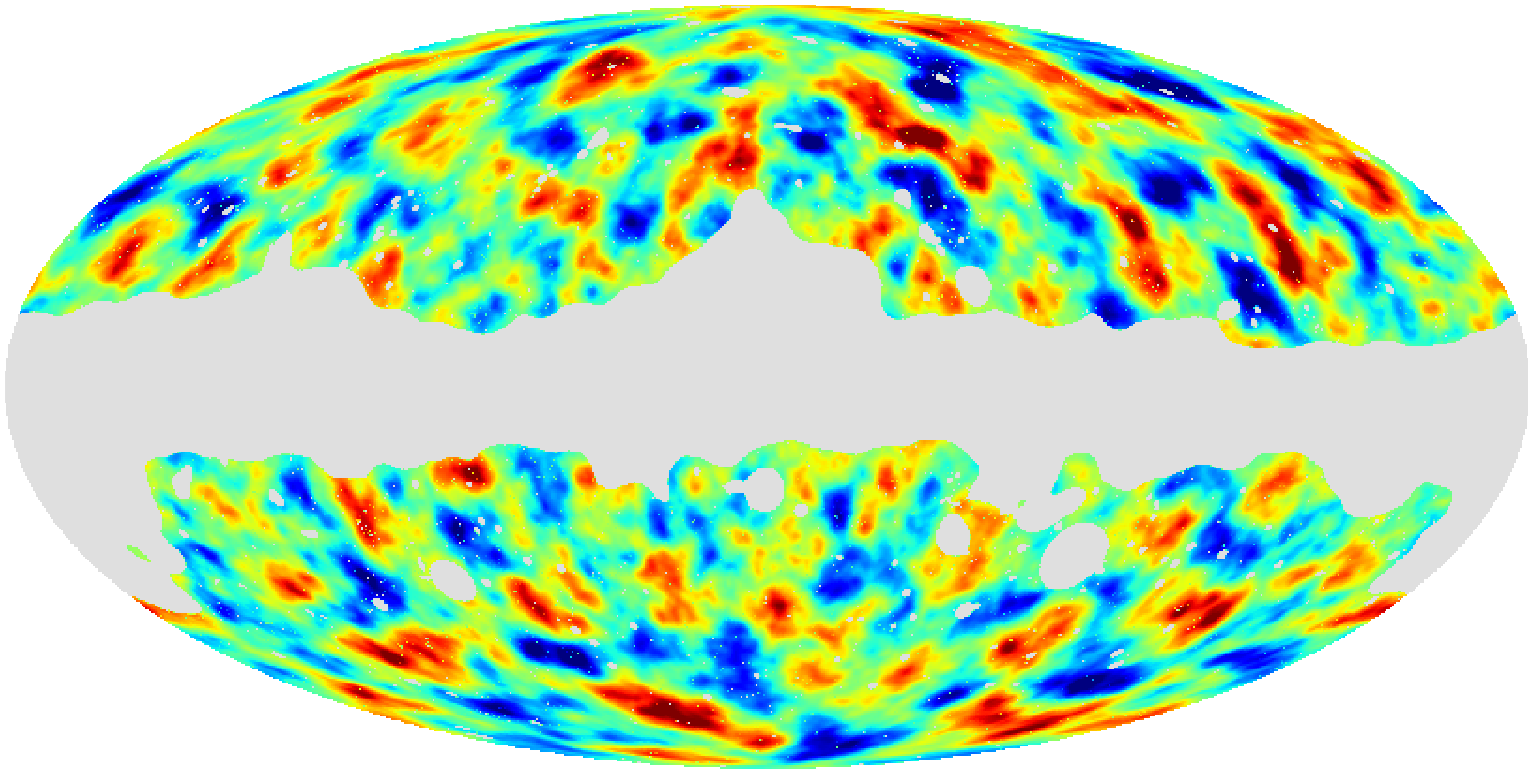

Planck lensing potential map: dark matter distribution at z~2

CMB lensing from Planck

mostly based on 2 Planck papers:

***Planck* 2015 results. XV. Gravitational lensing**

Lensing-induced *B*-mode map with Planck (internal reviewing)

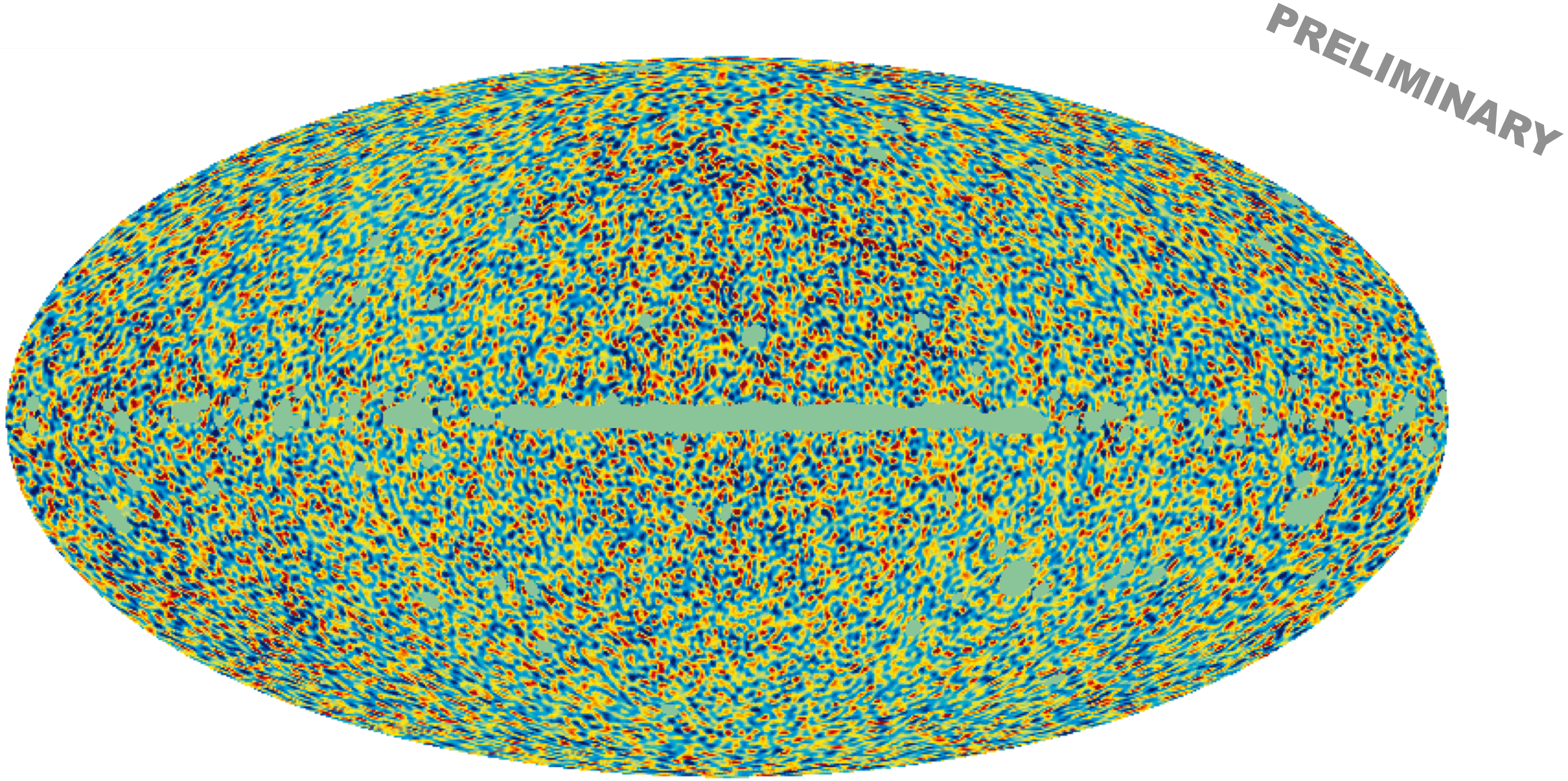

Planck lensing-induced B-mode map

CMB lensing from Planck

mostly based on 2 Planck papers:

Planck 2015 results. XV. Gravitational lensing

Planck Collaboration: P. A. R. Ade[91], N. Aghanim[64], M. Arnaud[78], M. Ashdown[74,6], J. Aumont[64], C. Baccigalupi[90], A. J. Banday[101,10], R. B. Barreiro[70], J. G. Bartlett[1,72], N. Bartolo[33,71], E. Battaner[103,104], K. Benabed[65,100], A. Benoît[62], A. Benoit-Lévy[25,65,100], J.-P. Bernard[101,10], M. Bersanelli[36,53], P. Bielewicz[101,10,90], A. Bonaldi[73], L. Bonavera[70], J. R. Bond[9], J. Borrill[15,95], F. R. Bouchet[65,93], F. Boulanger[64], M. Bucher[1], C. Burigana[52,34,54], R. C. Butler[52], E. Calabrese[98], J.-F. Cardoso[79,1,65], A. Catalano[80,77], A. Challinor[67,74,13], A. Chamballu[78,17,64], H. C. Chiang[29,7],
P. R. C … oulais[77],
B. P. … otti[49,90],
J. Delabrou … , X. Dupac[43],
G. Efstat … . Fraisse[29],
E. France … Nuevo[70,90],
K. M. Górsk … . Harrison[67,74],
S. Henr … olmes[72],
A. Horns … eihänen[28],
R. Ke … äki[2,48],
J.-M. Lama … I. Liguori[33,71],
P. B. Lilje … andolesi[52,34],
A. Ma … inhold[31],
A. Melchic … Montier[101,10],
G. Mo … erfield[21],
H. U. Nørg … Paoletti[52,54],
F. Pasian[5] … Pietrobon[72],
S. Plaszczy … . Rachen[22,84],
W. T. Reac … [2], C. Rosset[1],
M. Rossetti … avelainen[28,48],
G. Savini[88] … Sunyaev[84,94],
D. Sutton[67] … , M. Tucci[19],
J. Tuovi … Wehus[72],

The scientific results that we present today are a product of the Planck Collaboration, including individuals from more than 100 scientific institutes in Europe, the USA and Canada.

Planck is a project of the European Space Agency, with instruments provided by two scientific Consortia funded by ESA member states (in particular the lead countries: France and Italy) with contributions from NASA (USA), and telescope reflectors provided in a collaboration between ESA and a scientific Consortium led and funded by Denmark.

Outlines

- CMB lensing reconstruction: data and hint of methodology
- Lensing potential results
- Lensing potential implications for Cosmology
- Lensing-induced B-mode, results and implications

Gravitational Lensing by large-scale Structure

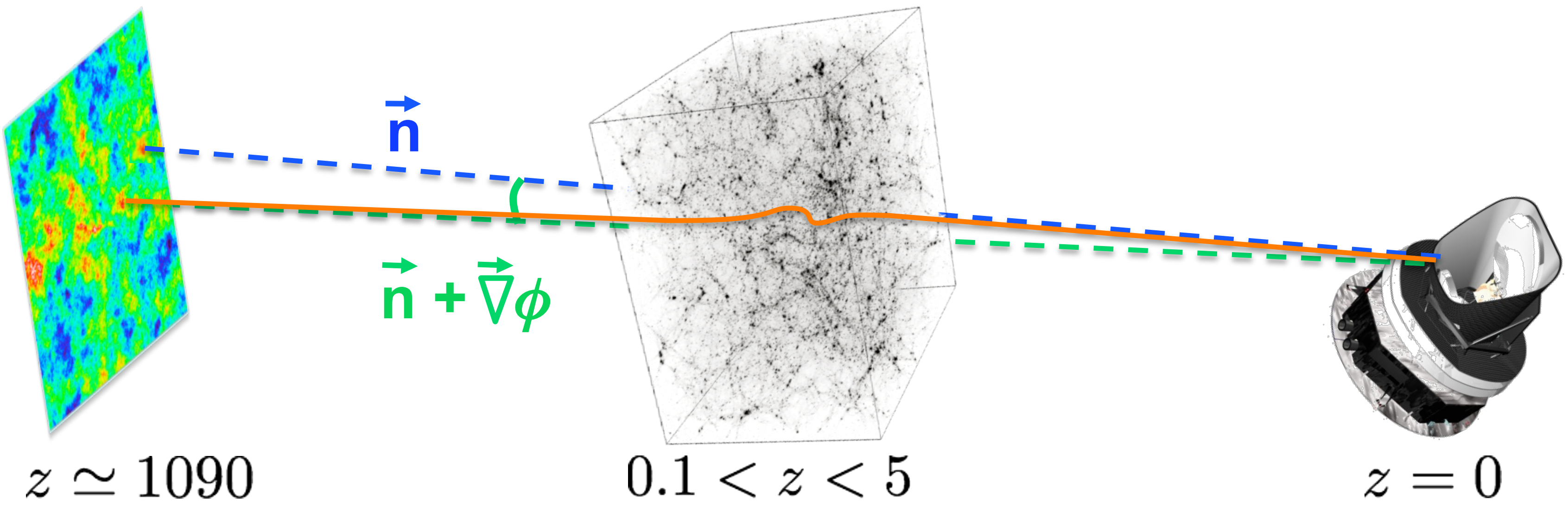

Remapping: $X(\mathbf{n}) = X^{\text{primo}}(\mathbf{n} + \nabla\phi(\mathbf{n})), \quad X \in \{T, Q \pm iU\}$

Lensing potential: $\phi(\hat{\mathbf{n}}) = -2\int_0^{\chi_*} d\chi \left(\frac{\chi_* - \chi}{\chi_*\chi}\right)\Psi(\chi\hat{\mathbf{n}}; \eta_0 - \chi)$

- max. efficiency at z~2
- typical size ~300 Mpc
- linear growth

kernel in a flat universe — conformal distance — lookback conformal time

Observational signature

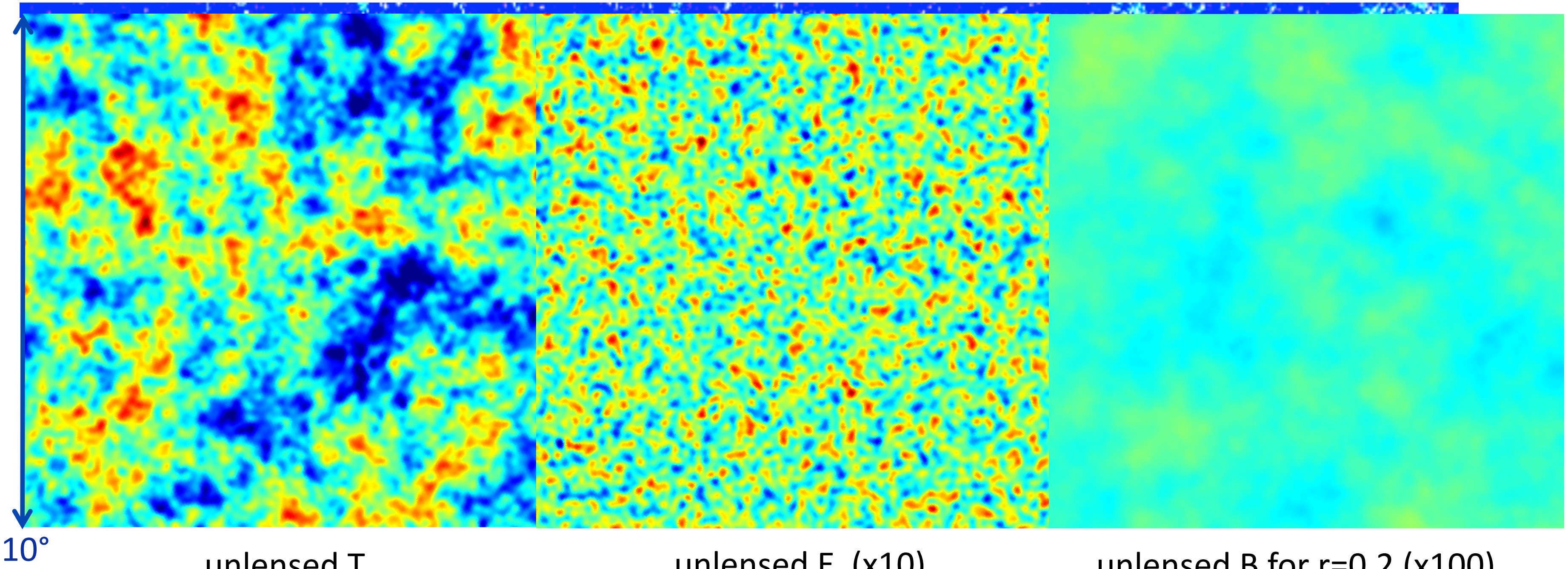

unlensed T　　unlensed E (x10)　　unlensed B for r=0.2 (x100)

Lensing typical scales:

- deflection scale $\simeq$ 2.5 arcmin (rms)
- correlation length $\simeq$ 2 degrees

Signatures:

- power spectra smoothing ($\simeq$10% at high-l)
- secondary B-mode (dominates at l > few 100)
- inducing NG

$$\delta X(\mathbf{n}) \sim \nabla\phi(\mathbf{n}) \cdot \nabla X^{\rm primo}(\mathbf{n}), \quad X \in \{T, Q \pm iU\}$$

Using the NG signature in the maps, the underlying phi potential can be reconstructed

Observational signature

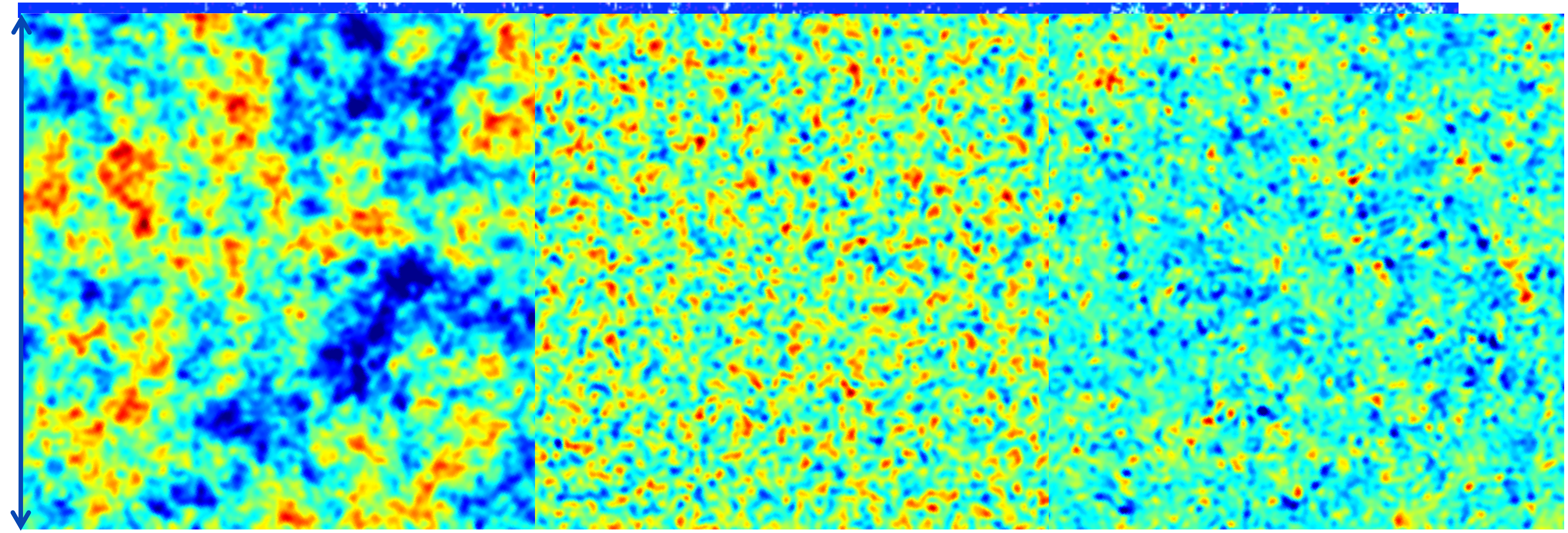

Lensing typical scales:

- deflection scale $\simeq$ 2.5 arcmin (rms)
- correlation length $\simeq$ 2 degrees

Signatures:

- power spectra smoothing ($\simeq$10% at high-l)
- secondary B-mode (dominates at l > few 100)
- inducing NG

$$\delta X(\mathbf{n}) \sim \nabla\phi(\mathbf{n}) \cdot \nabla X^{\rm primo}(\mathbf{n}), \quad X \in \{T, Q \pm iU\}$$

Using the NG signature in the maps, the underlying phi potential can be reconstructed

CMB Lensing Reconstruction Basics

ϕ map reconstruction using *quadratic estimators*

T. Okamoto & W. Hu [astro-ph/0301031]

$$\hat{\phi}^{(XZ)}_{LM} = A^{(XZ)}_{L} \sum_{\ell_1 m_1} \sum_{\ell_2 m_2} \mathcal{G}^{(XZ)}_{LM\ell_1 m_1 \ell_2 m_2} \; \bar{X}_{\ell_1 m_1} \bar{Z}_{\ell_2 m_2} \qquad (X,Z) \in \{T,E,B\}$$

filtered versions of {T, E, B} maps

normalisation and filters optimisation → unbiased, minimum variance estimator

NB: tractable computation in real-space : $\hat{\phi}^{(XZ)}_{LM} = A^{(XZ)}_{L} \int d\mathbf{n} \, \nabla_{\mathbf{s}} Y^{*}_{LM}(\mathbf{n}) \cdot [\bar{X}(\mathbf{n}) \nabla_{\mathbf{s}} \bar{\bar{Z}}(\mathbf{n})] \quad (X,Z) \in \{T, Q \pm iU\}$

$$\hat{\phi}^{(\mathrm{mv})}_{LM} = \sum_{XZ} w^{XZ}_{L} \, \hat{\phi}^{(XZ)}_{LM}$$

Minimum-Variance combination (TT, TE, EE, EB, TB)

$\hat{C}^{\phi\phi}_{L}$ reconstruction using the 4-point correlator information

$$\hat{C}^{\phi}_{L} = \frac{1}{(2L+1)} \sum_{M} |\hat{\phi}_{LM}|^2 - N^{(0)}_{L} - \mathcal{O}(C^{\phi}_{L})$$

Gaussian bias: disconnected part of the 4-pt correlator

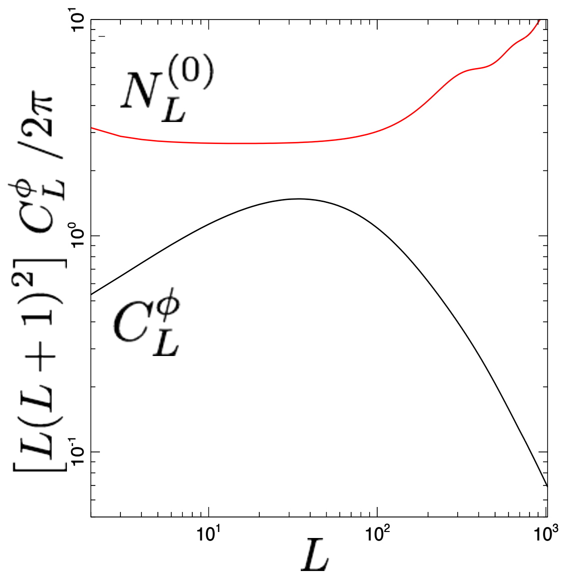

Reconstruction from the data

1. data processing steps from timelines to map are critical

- TOI-processing
- Map-making

Planck 2013 results. II-X

Planck 2015 results. II-VIII

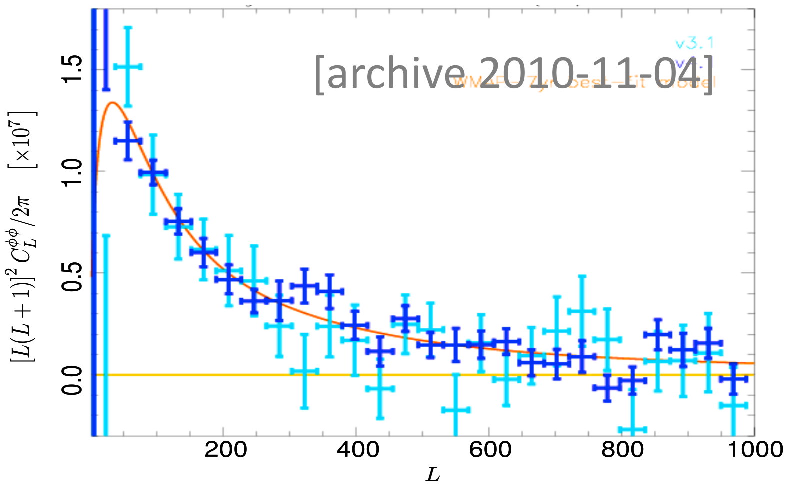

Early full-sky reconstructions on the same amount of data

- *better model of the time transfert function*
- NL-correction in the V->W
- better SSO flagging
- improved 4K-lines corr.
- better glitches removal

2. Astrophysical foregrounds are the major concern

We exploit Planck frequency coverage to clean them (component separation)

Masks:

- detected point sources
  - radio/IR galaxies using PCCS I/II Planck 2013 results. XXVIII / 2015
  - SZ clusters using PCC I/II Planck 2013 results. XXIX / 2015 XXVII
  - Cold Cores using CC I/II Planck Early Results. VII / 2015 XXVIII
- diffuse emission
  - galactic plane Planck 2013 results. XII / 2015 X
  - CO regions Planck 2013 results. XIII / 2015 VIII

→ masks induce the dominant bias at ϕ map level

Reconstruction from the data

Debiasing at the map level :

Any effects breaking the spatial isotopy of the maps (e.g. masks, inhomogeneous noise) induce spurious ϕ
Bias correction using Monte-Carlo simulation (that includes all known bias sources) :

$$\hat{\phi}^{(c)} = \hat{\phi} - < \hat{\phi} >_{\mathrm{MC}}$$

Our power spectrum estimator :

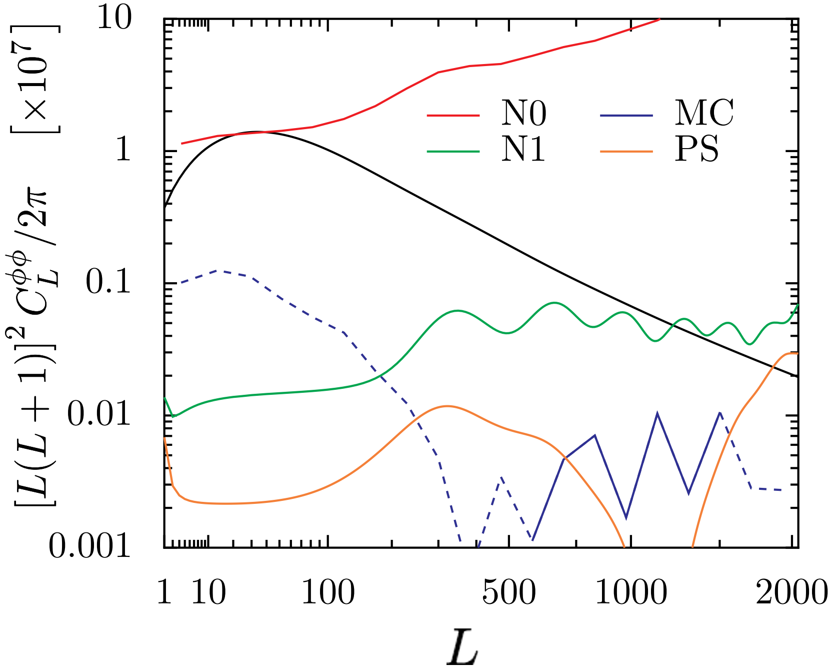

$$\hat{C}_L^{\phi} = \frac{1}{(2L+1) f_{\mathrm{sky}}} \sum_M |\hat{\phi}_{LM}^{(c)}|^2 - N_L^{(0)}$$

$-N_L^{(1)}$ the $\mathcal{O}(C_L^{\phi\phi})$ term

$-N_L^{(\mathrm{MC})}$ residual bias from *lensed* MC simulation

$-N_L^{(\mathrm{ps})}$ (small) point source shot-noise trispectrum

Data (2013 vs 2015)

Planck lensing 2013 baseline T map:

- 15.5 months of data integration
- MV combination of 143 and 217 GHz maps
- corrected for a dust template using the 857GHz map
- $\simeq$ 60% of the sky (after apodization)

Planck lensing 2015 baseline {T, Q, U} maps:

- about 30 months of data
- foreground cleaned maps using SMICA
- ICA using the 9 frequency maps

  Planck 2015 results. XII

- $\simeq$ 70% of the sky
- bandpass filtering $100 \leq \ell \leq 2000$

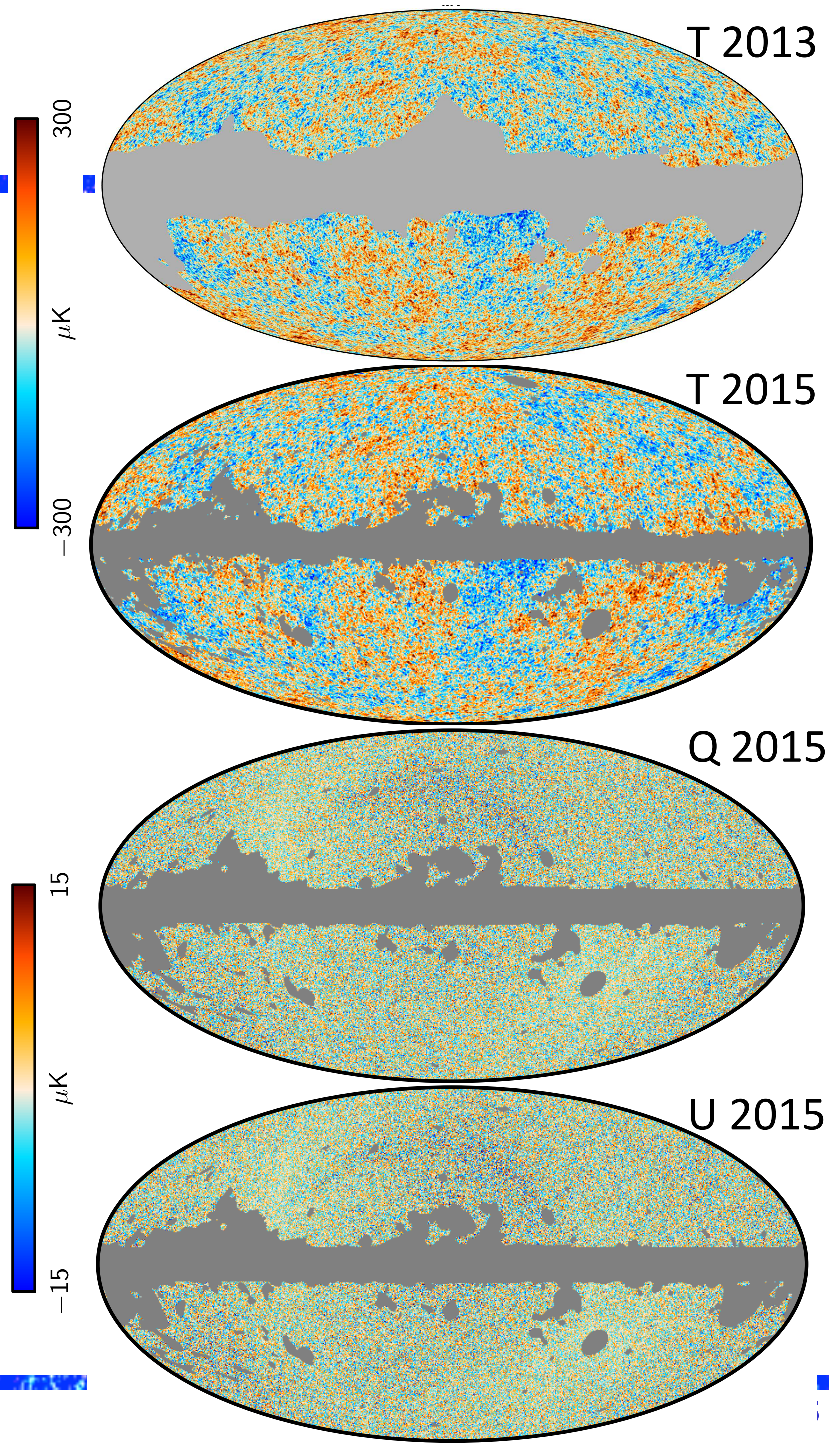

Reconstructed ϕ map

TT 2013

see Lewis talk
Ferrara 2014

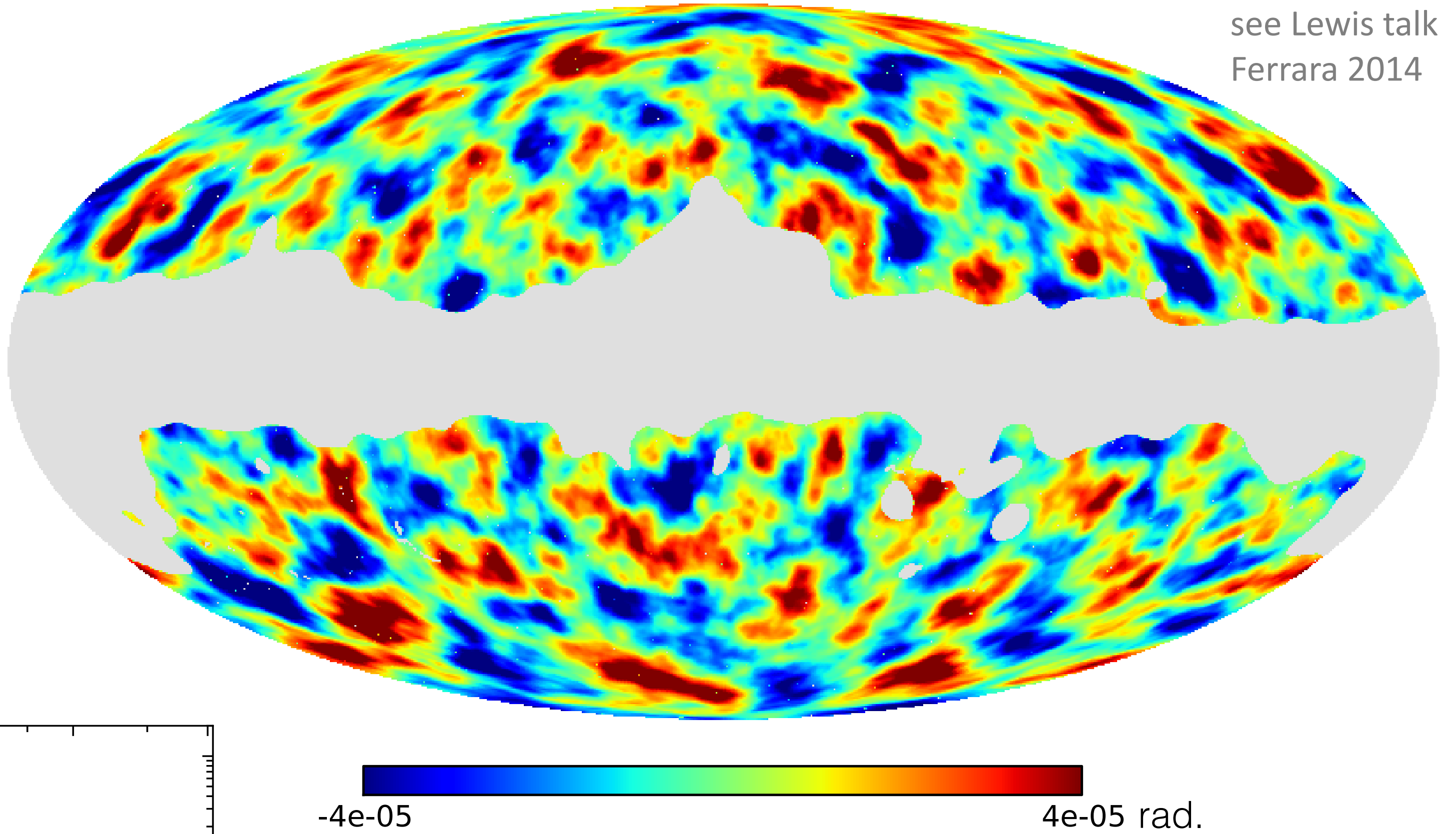

dominant noise

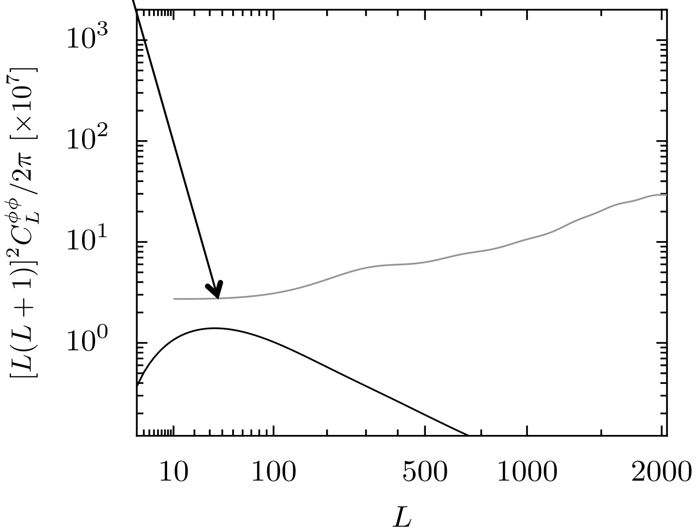

noise-dominated map of the dark matter around z=2

Reconstructed ϕ map

TT 2015

see Lewis talk
Ferrara 2014

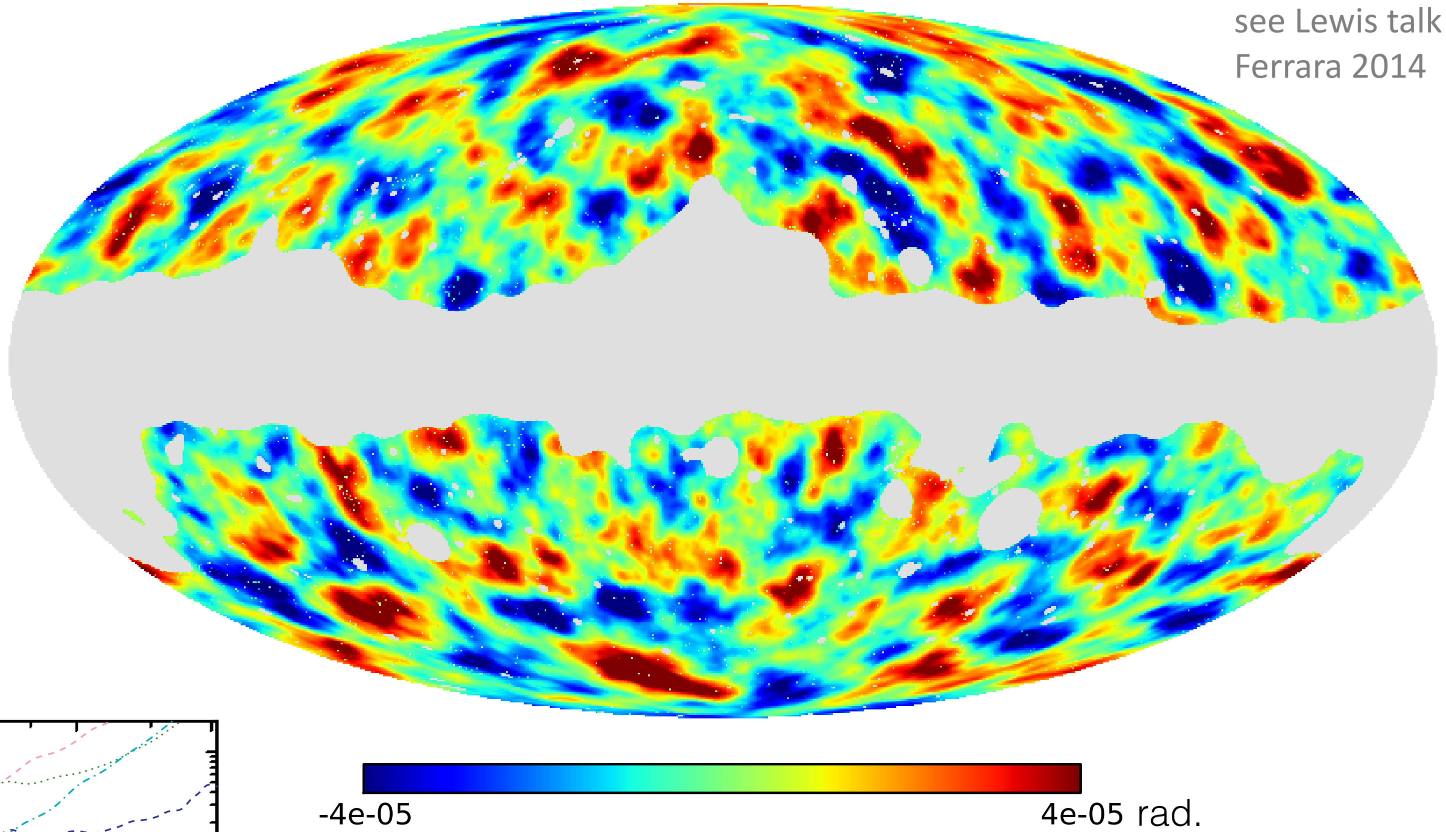

dominant noise

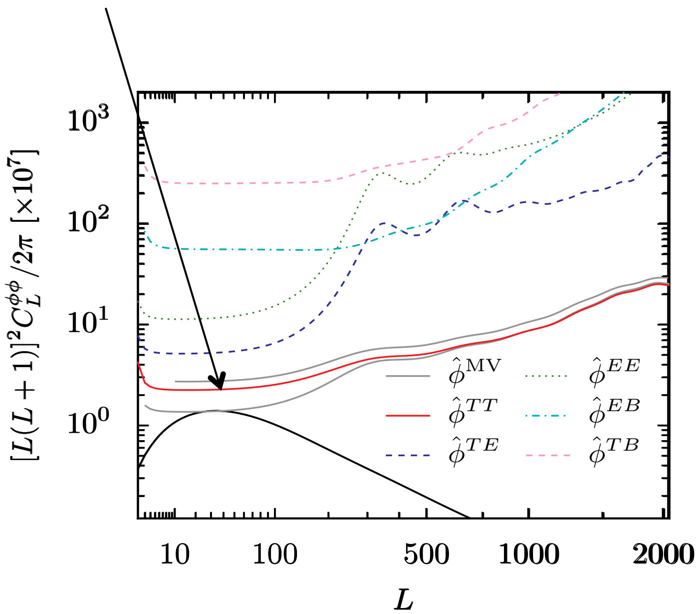

twice the amount of data

25% improvement of the noise level

(part of the noise are temperature anisotropy cosmic variance)

Reconstructed ϕ map

TE 2015

see Lewis talk
Ferrara 2014

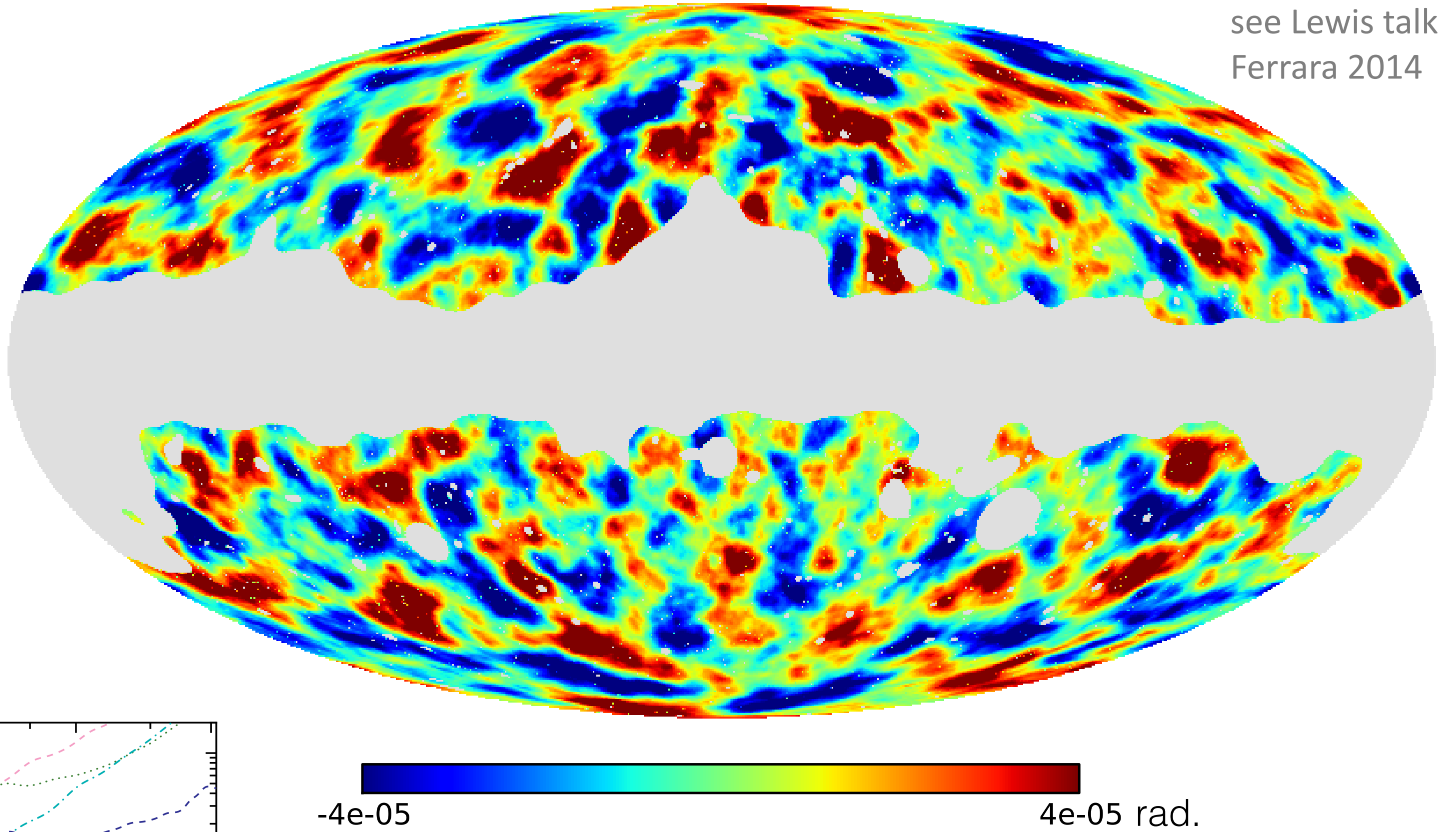

dominant noise

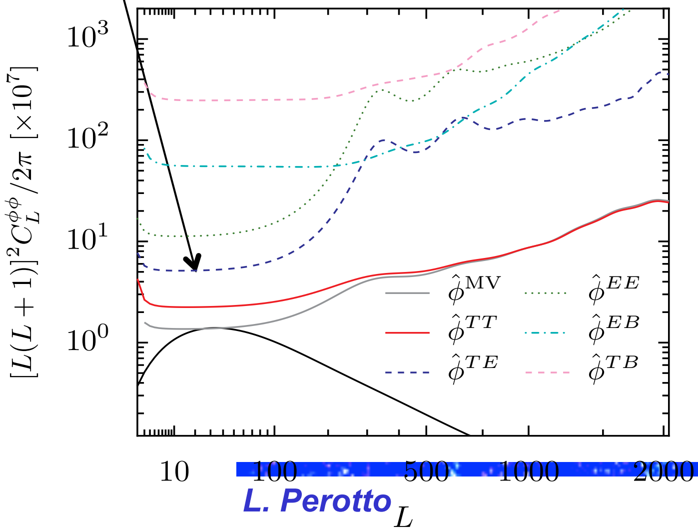

another 25% improvement coming from the polarization, mainly TE

Reconstructed ϕ map

EE+EB 2015

see Lewis talk
Ferrara 2014

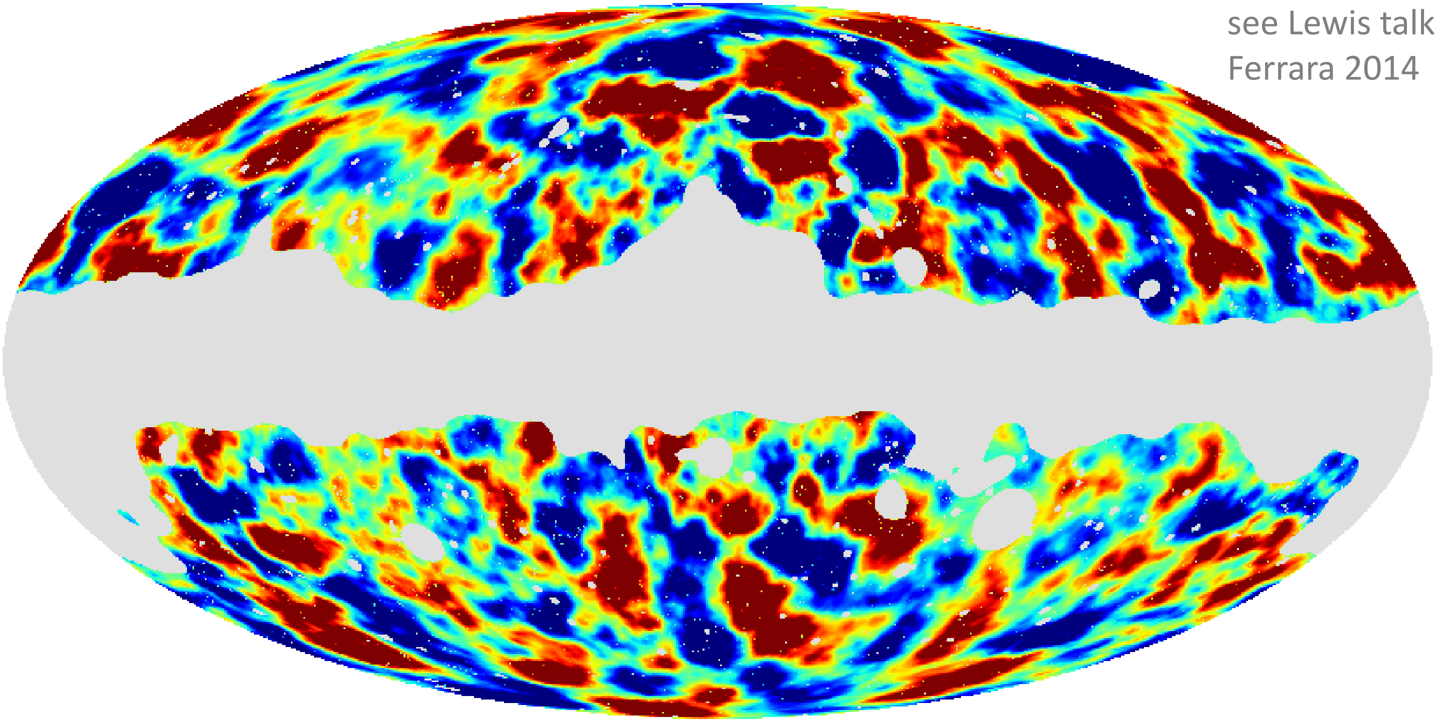

dominant noise

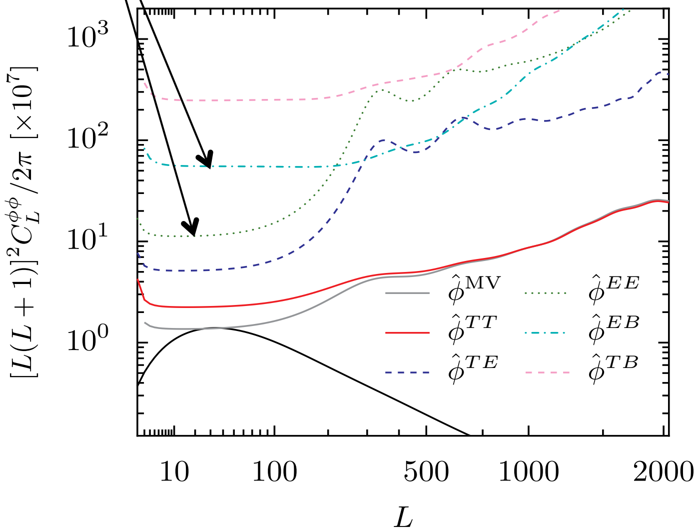

significant measurement using polarization only

Reconstructed ϕ map

see Lewis talk
Ferrara 2014

MV 2015

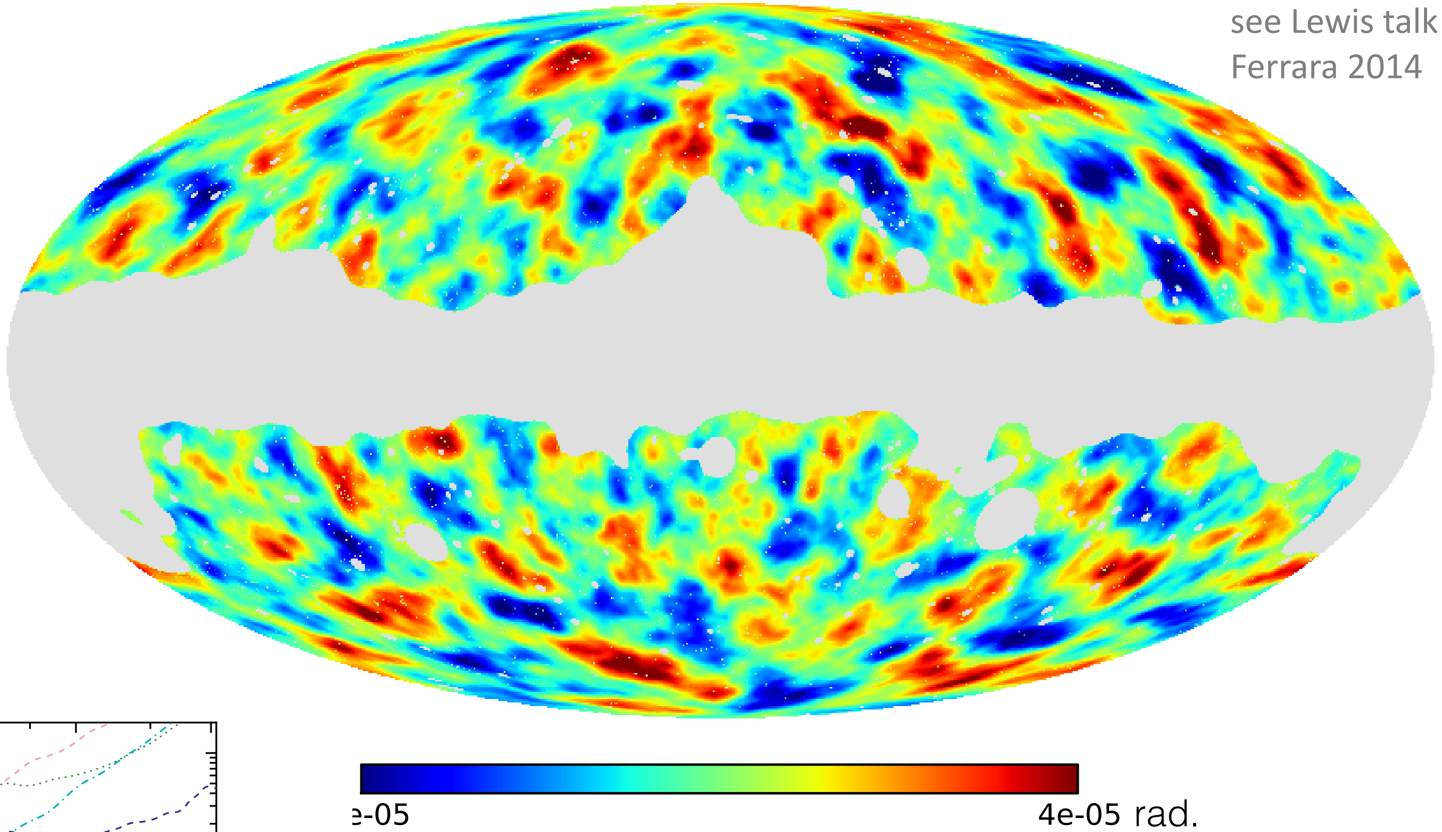

dominant noise

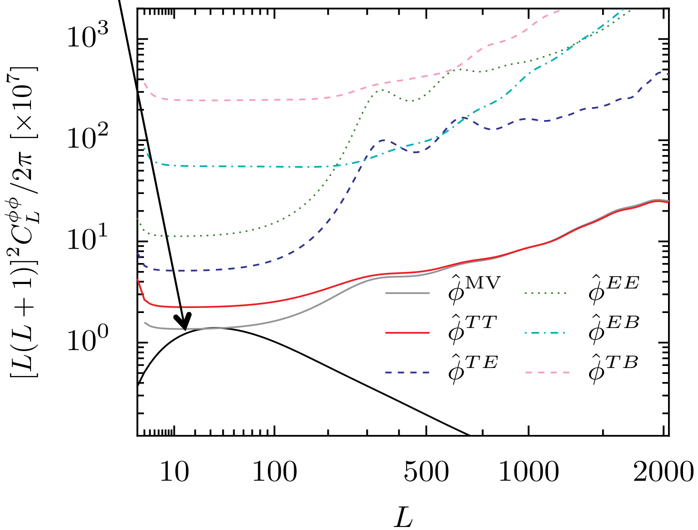

50% improvement of the noise level w.r.t. 2013

$S/N \lesssim 1$ map of the dark matter around z=2

highly correlated with other large scale structure probes

Correlation with other LSS tracers

External data

Planck 2014 XVII (Lensing)

- 20 sigma correlation with NVSS radio galaxies and quasars (z_{mean} = 1.1)
- 10 sigma with SDSS Luminous Red Galaxies (z_{mean} = 0.55)
- 7 sigma with the WISE satellite IR galaxies catalog (z_{mean} = 0.1)

Planck's Cosmic Infrared Background (CIB)

- unresolved high-redshift dusty star-forming galaxies
- dominant extra-galactic emission at $\geq$ 353GHz

- first detection (42 sigma) of a correlation between 545GHz T and lensing maps :

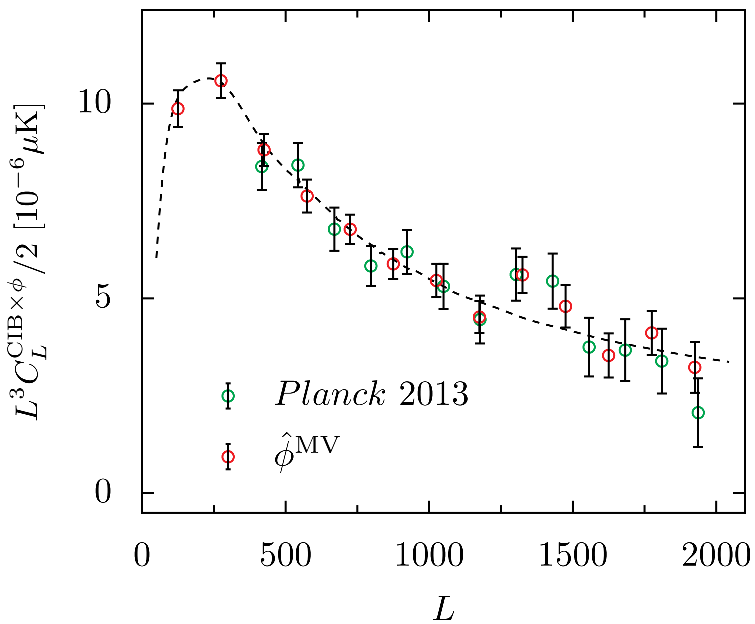

Stacking of the ϕ map at the location of :

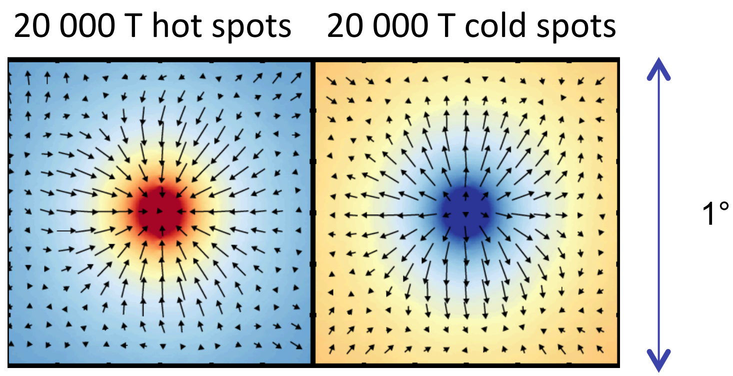

Planck 2014 XVIII (CIB-Lensing)

- helps in probing the origin of the CIB hence in constraining the star formation history

Correlation with the ISW effect

ISW: Integrated Sachs-Wolfe effect

- At late-time, gravitational potentials induce a secondaries

$$\frac{\Delta T}{T_{\rm CMB}} = \frac{2}{c^3}\int_{\eta_*}^{\eta_0} d\eta \frac{d\Psi}{d\eta}$$

- that correlate to the ϕ map

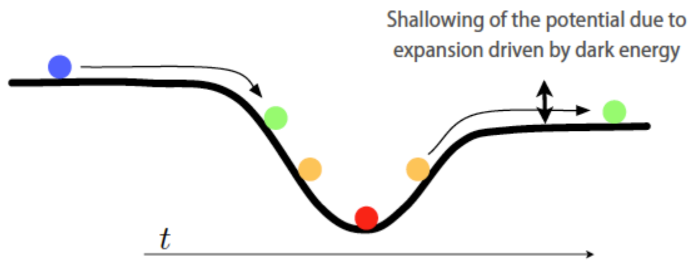

credit K. Benabed ESLAB 2013

ISW results Planck 2015 results XXI (ISW)

Planck T x ϕ : 3σ detection (20% improvement wrt 2013)

Planck T x LSS : 2.9σ detection

Joint : 4σ detection

ISW-lensing bispectrum (Tϕ cross-correlation)

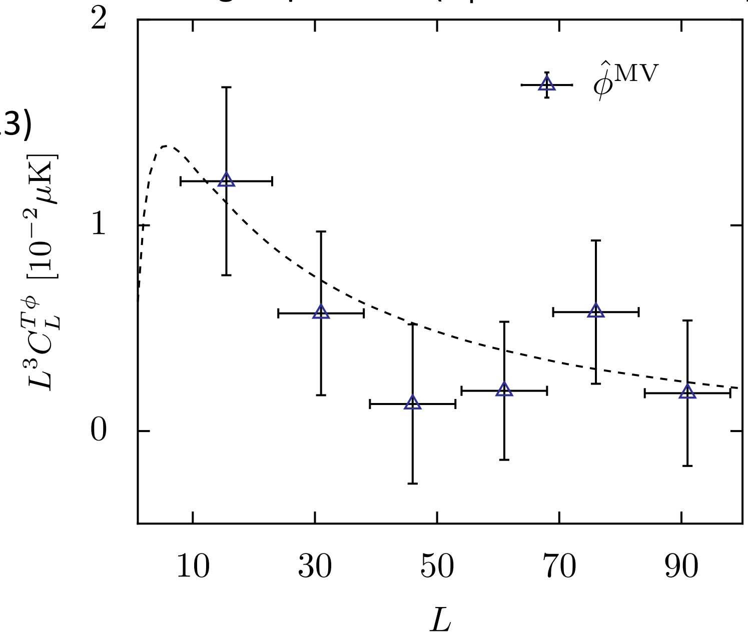

Implications

- 3 σ detection of Ω_Λ
- important bias to the CMB primordial non-Gaussianity (from inflation) that must be subtracted
  Planck 2015 results XVII (non-Gaussianity)

Other cross-correlation studies

Further cross-correlation between the released 2013 and 2015 ϕ maps to the community and…

- Thermal SZ (detection at 6.2 σ)

  Detection of Thermal SZ -- CMB Lensing Cross-Correlation in Planck Nominal Mission Data,
  J. Colin Hill, David N. Spergel, arXiv:1312.4525

- Herschel selected galaxies at z > 1.5 (detection at 20 σ)

  Cross-correlation between the CMB lensing potential measured by Planck and high-z sub-mm galaxies detected by the Herschel-ATLAS survey,
  F. Bianchini, P. Bielewicz, A. Lapi, J. Gonzalez-Nuevo, C. Baccigalupi, G. de Zotti, et al. arXiv:1410.4502

- Fermi-LAT γ-ray map (detection at 3 σ)

  Evidence of cross-correlation between the CMB lensing and the gamma-ray sky,
  N. Fornengo, L. Perotto, M. Regis, S. Camera, arXiv:1410.4997

- CFHTLenS galaxy number density

  Cross-Correlation of CFHTLenS Galaxy Number Density and Planck CMB Lensing,
  Y. Omori, G. Holder, arXiv:1502.03405

- CFHTLenS weak lensing

  Cross-correlation of Planck CMB Lensing and CFHTLenS Galaxy Weak Lensing Maps, Jia Liu, J. Colin Hill, arXiv:1504.05598

Main result: the lensing power spectrum

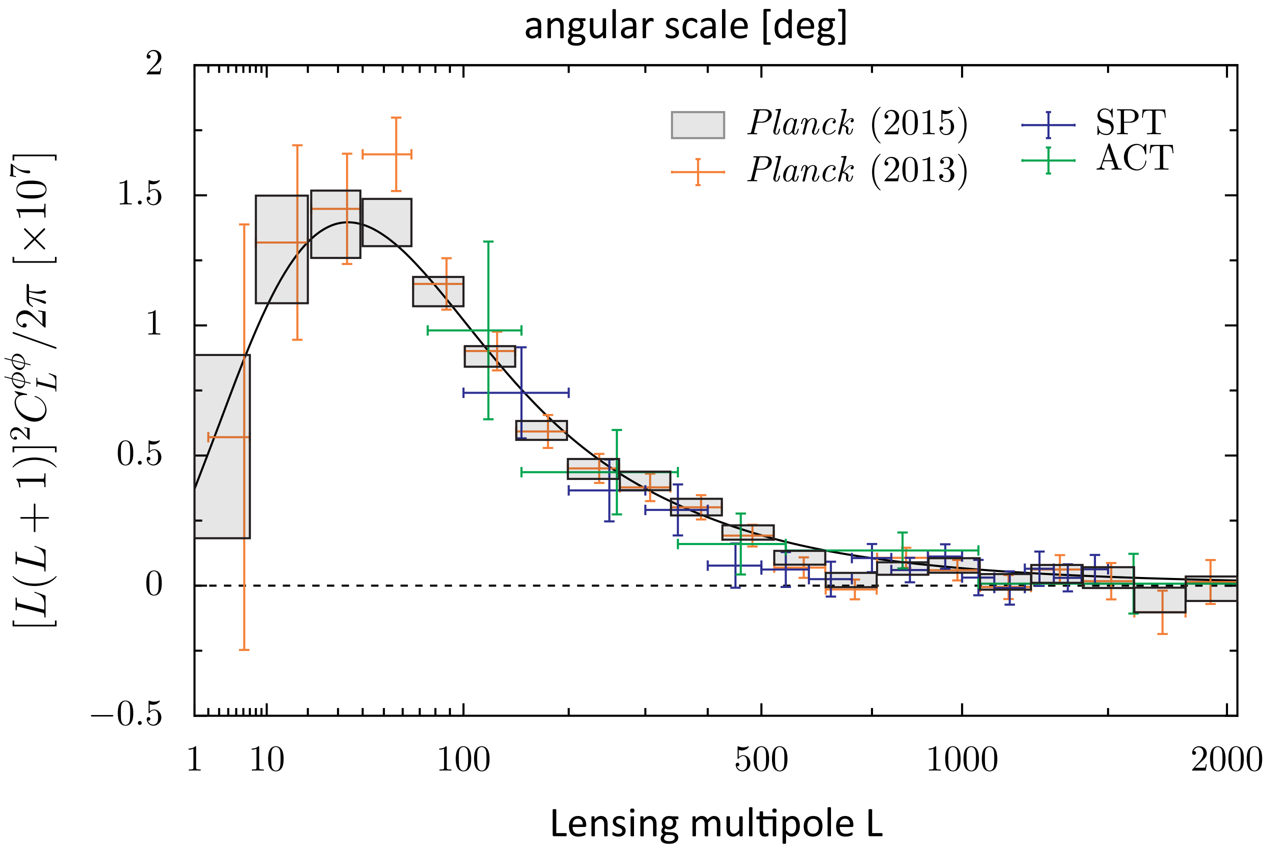

Planck 2013 : $A_{\rm lens} = 0.943 \pm 0.040$ (25σ detection)

Planck 2015 : $A_{\rm lens} = 0.987 \pm 0.025$ (40σ detection)

Individual estimators

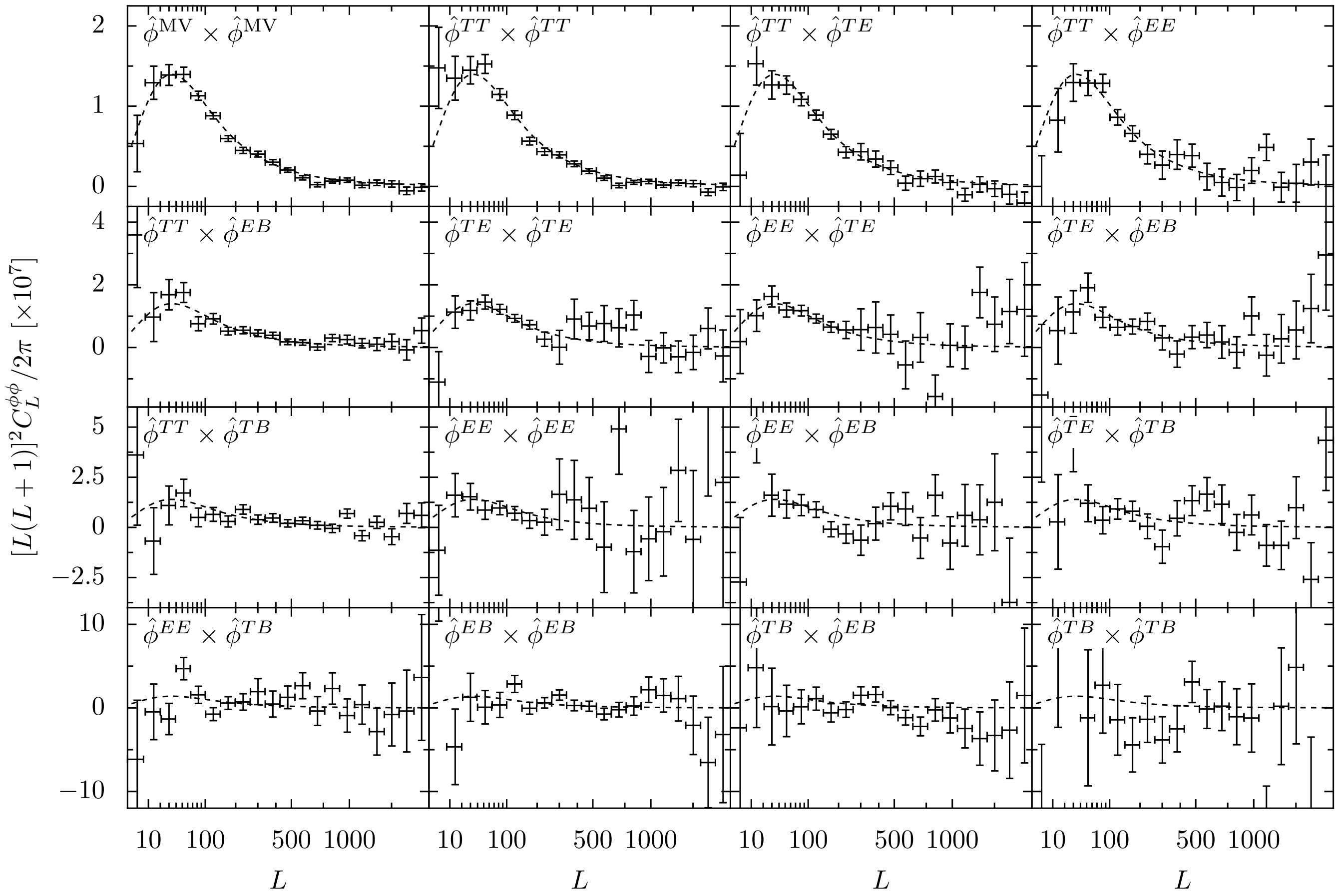

15 consistent ϕϕ measurements
dominant contribution from TT and TE

Robustness tests

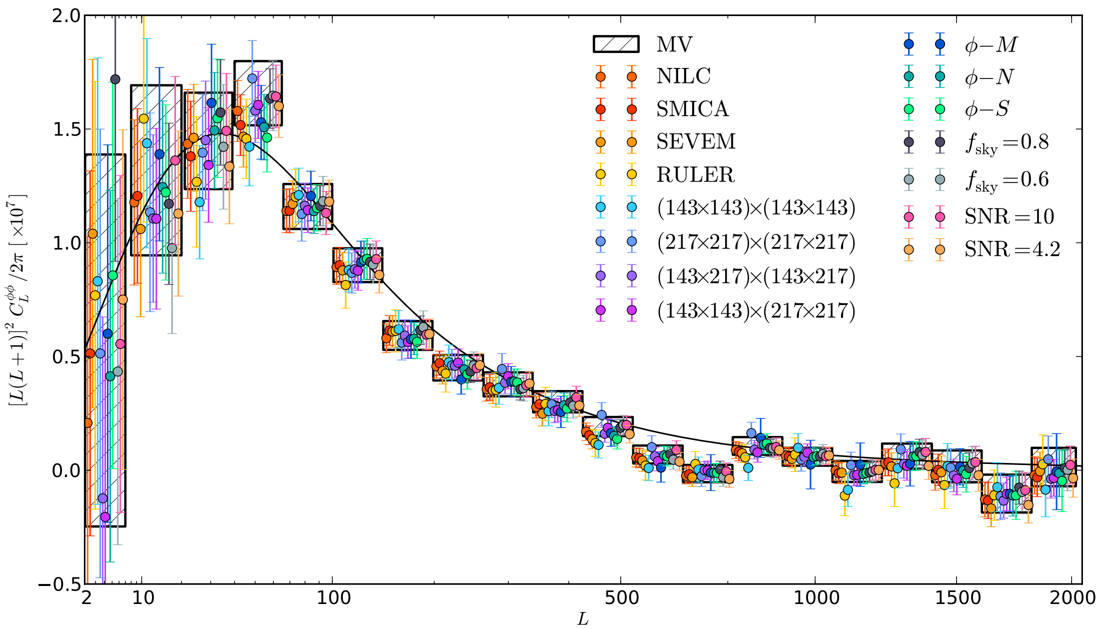

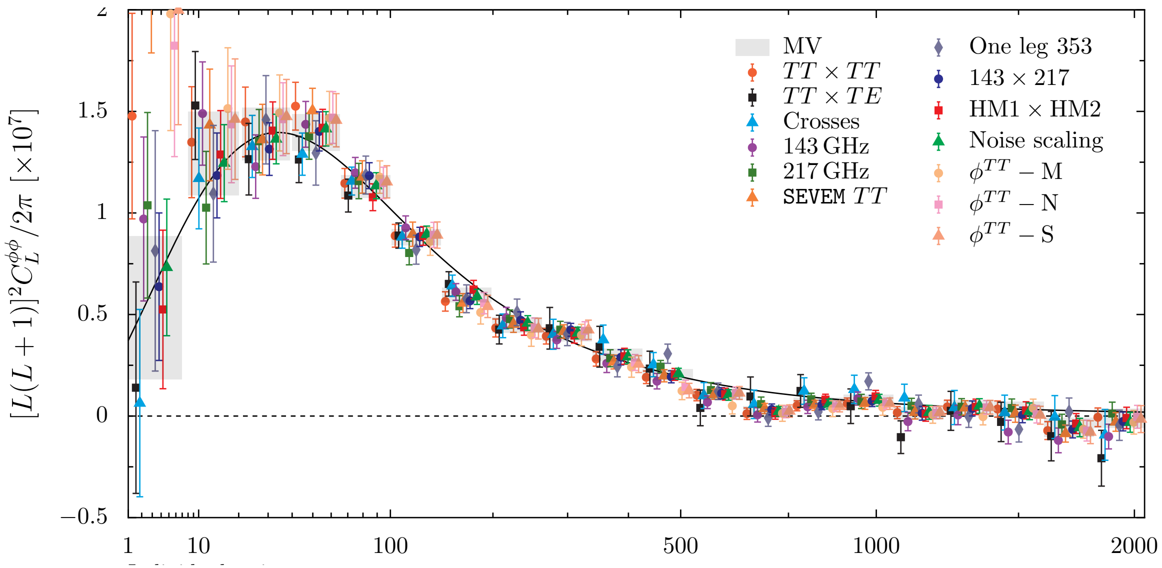

As in 2013, the 2015 results pass a wealth of consistency checks including:

- robustness to foregrounds
- data splitting consistency
- robustness to bias at map-level

The conservative case

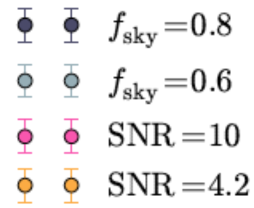

2013

Comparison to results using different galactic/point sources masks (baseline : fsky=0.7, SNR=5)

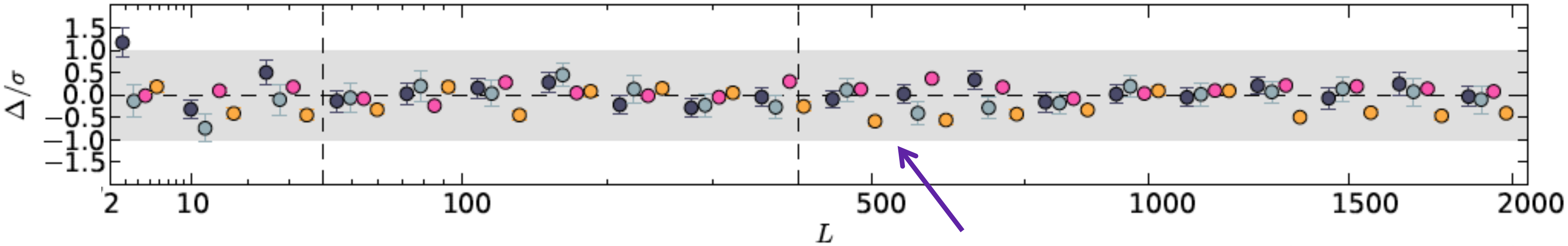

larger scatter than expected (from MC sims)

2015

curl-modes null test

Namikawa et al. [astro-ph/1110.1718]

$\mathbf{d} = \nabla\phi$: curl-free

we construct an estimator of $\mathbf{d}^{\rm curl} = \star\nabla\psi$

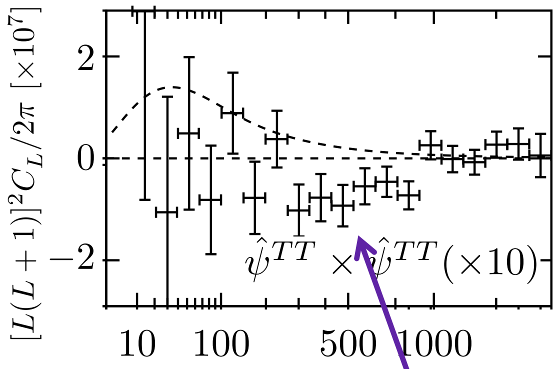

~ 3σ non-zero feature over 400<L<2000

L = 8 | Large map-level debiasing | 40 | **conservative interval** • used for Cosmology • retains 90% of the S/N | 400 | Large $N_L^{(0)}$ correction | 2000

Outlines

- CMB lensing reconstruction: data and hint of methodology
- Lensing potential results
- Lensing potential implications for Cosmology
- Lensing-induced B-mode, results and implications

Consistency with the Planck base LCDM model

• Measure of a freely floating A that scales $C_L^{\phi\phi}$

$$A_{\rm lens} = 0.95 \pm 0.04 \quad \text{Planck TT + lowP + lensing}$$

LCDM6 model: good description of the universe at $z \leq 5$

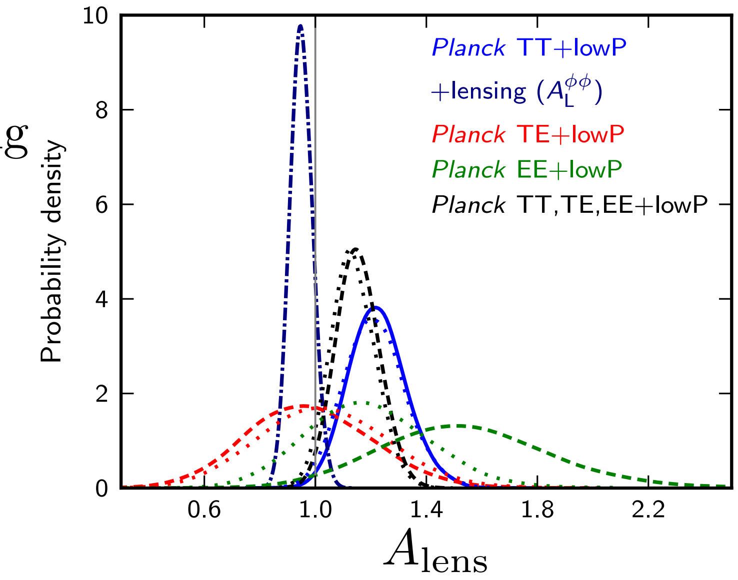

• Measure of a freely floating A that scales the lensing smoothing of Cl^{TT}, Cl^{TE}, Cl^{EE}

$$A_{\rm lens}^{\rm smooth} = 1.22 \pm 0.10 \quad \text{Planck TT + lowP}$$

C_l^{TT} favors higher lensing power amplitude
to accomodate the tension to the « 20<l<30 dip »

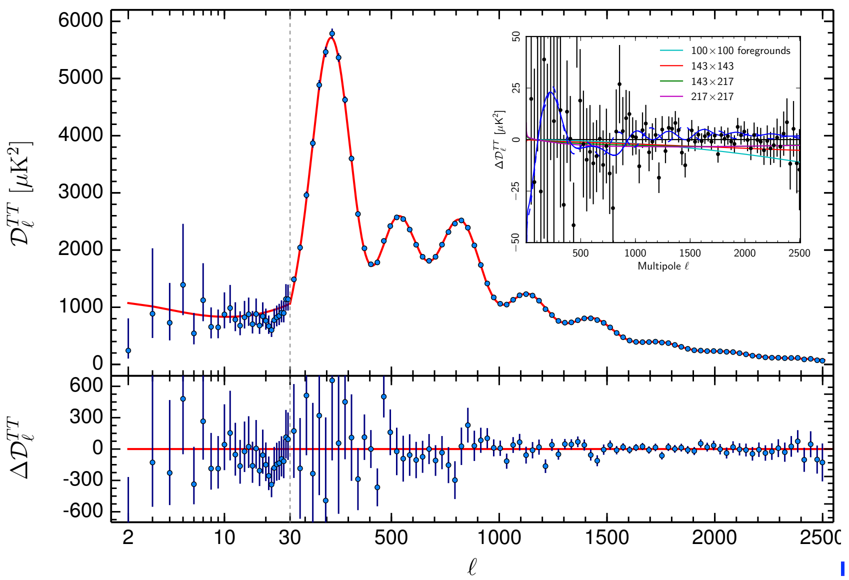

Constraints on the LCDM model

Information on the matter up to last-scattering $\Rightarrow$ constraints on the post-recombination evolution

- LCDM constraints from CMB lensing alone

Clϕϕ depends mainly of $A_s\,,\quad \ell_{eq} \equiv k_{eq}\chi_* \overset{\omega_r\,\text{fixed}}{\propto} (\Omega_m h^2)^{1/2}$

constrains the subspace $\{\sigma_8,\quad \Omega_m,\quad H_0\}$

a well determined parameter $\sigma_8\Omega_m^{1/4} \approx \left(A_s \ell_{eq}^{2.5}\right)^{1/2}$

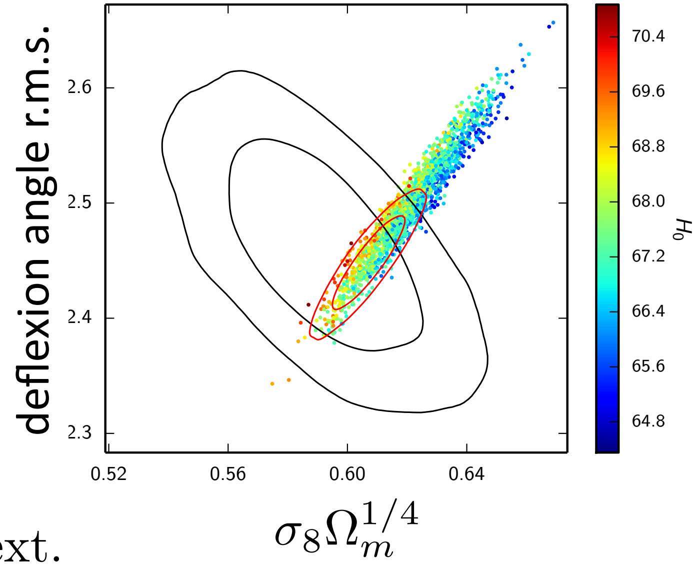

$$\sigma_8 = 0.829 \pm 0.014 \quad \text{Planck TT + lowP}$$
$$\sigma_8 = 0.815 \pm 0.009 \quad \text{Planck TT + lowP + lensing}$$

$$H_0 = 67.3 \pm 1.0 \quad \text{Planck TT + lowP}$$
$$H_0 = 67.8 \pm 0.9 \quad \text{Planck TT + lowP + lensing}$$
$$H_0 = 67.9 \pm 0.5 \quad \text{Planck TT + lowP + lensing + ext.}$$

(mild precision / important accuracy improvement)

- Reionization optical depth constraints

Primordial TT alone depends on $A_s e^{-2\tau}$

$$\tau = 0.078 \pm 0.019 \quad \text{Planck TT + lowP}$$
$$\tau = 0.070 \pm 0.024 \quad \text{Planck TT + lensing}$$
$$\tau = 0.066 \pm 0.013 \quad \text{Planck TT + lensing + BAO}$$

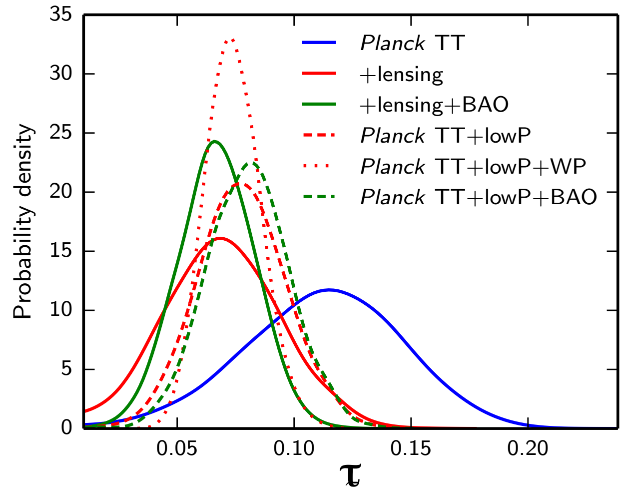

Good agreement with low-ell polar and BAO

Constraints on extension to the base LCDM model

- Geometrical degeneracy breaking in a non-flat Universe

CMB alone (Planck TT + lowP + lensing)

- imposes a flat-geometry at sub-percent level;
- x3 improvement of errors over TT+lowP alone
- $\lesssim 3\sigma$ evidence of Dark Energy

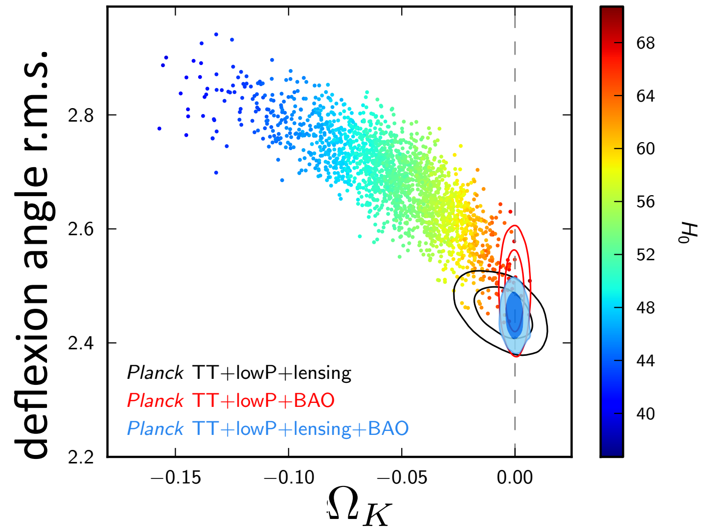

- Constaints on the neutrino sector

- for $\sum_\nu m_\nu \lesssim 1.3\,\mathrm{eV}$ (i.e. ν still relativistic at recombinaison): tiny constraints from TT alone
- oscillation measure: $\sum m_\nu \geq 0.06\,\mathrm{eV}$
at least 2 ν non-relativistic (NR) today

- After the NR transition: contribution to the expansion rate but not to the clustering of small-scale structure.

- Step-like signature in $C_L^{\phi\phi}$

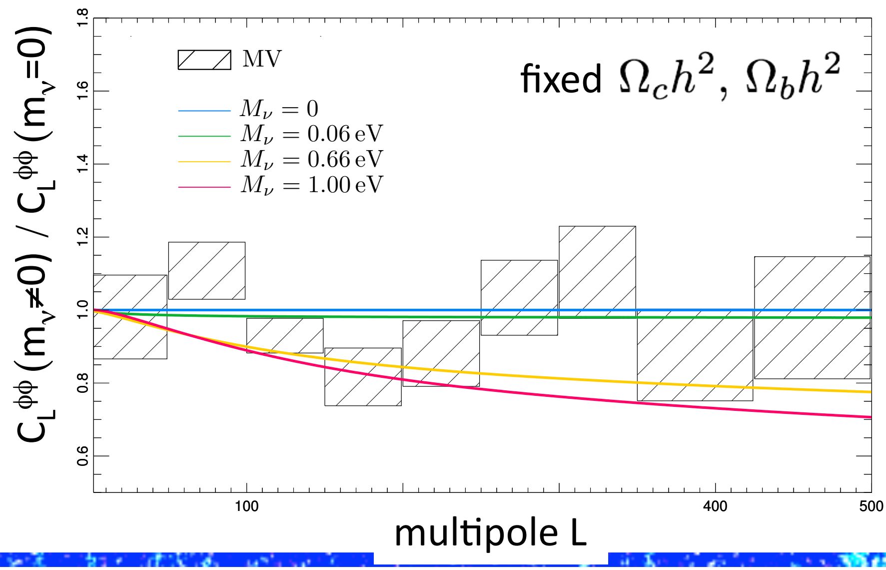

Constraints on neutrino masses

In a $\Lambda\mathrm{CDM6} + \sum_\nu \mathrm{m}_\nu$ model with $N_{\mathrm{eff}} = 3$ degenerate massive neutrinos:

$$\sum m_\nu < 0.72 \quad 95\%; \ \mathrm{Planck\,TT + lowP}$$

$$\sum m_\nu < 0.68 \quad 95\%; \ \mathrm{Planck\,TT + lowP + lensing}$$

mild improvement (whereas we expected a x2 improvement !)

Explanation: a combination of 2 effects:

- TT disfavors large m_ν

  large m_ν yields

  ➔ lower lensing smoothing

  ➔ less level-arm to accomodate to the « low-ell dip »

- ϕϕ autorises large m_ν

  slight trough at around L=200

Best limit:

$$\sum m_\nu < 0.23 \quad 95\%; \ \mathrm{Planck\,TT + lowP + lensing + external\,data}$$

Outlines

- CMB lensing reconstruction: data and hint of methodology
- Lensing potential results
- Lensing potential implications for Cosmology
- Lensing-induced B-mode, results and implications

Lensing-induced B-mode

- lensing-B polarization maps:

At first-order in ϕ

$$\left(Q^{\rm lens} \pm iU^{\rm lens}\right) = \nabla\left(Q^{\rm primo} \pm iU^{\rm primo}\right) \cdot \nabla\phi$$

$$B^{\rm lens}_{\ell m} = \sum_{LM}\sum_{\ell' m'} \phi_{LM} E^{\rm primo}_{\ell' m'}\ \mathcal{G}^{mMm'}_{\ell L \ell'}$$

W. Hu [astro-ph/0001303]

A lensing-B map template can be synthesized using
• the PLANCK polarization maps (keeping pure E-mode contribution)
• and PLANCK lensing potential estimate (or another ϕ tracer)

- lensing-B power spectrum:

When cross-correlated to the observed polarization maps, the lensing-B polarization maps provide a lensing B-mode power spectrum measurement :

$$\hat{C}^{B_{\rm lens}}_{\ell} = \frac{f_{\rm sky}^{-1}}{2\ell+1}\sum_m B^*_{\ell m}\hat{B}^{\rm lens}_{\ell m}$$

The lensing-B synthesis methods

We developped 2 independent methods…

main difference in the sky cuts treatment; different implementions / same mathematics

- spherical-harmonics space-based method
  - used in the Planck 2015 lensing paper
  - mask treatment: minimum-variance filtering of T and P
  - based on the baseline lensing extraction of Planck 2015 lensing

$$\hat{B}^{\rm lens}_{\ell m} = \mathcal{B}^{-1} \sum_{LM} \sum_{\ell' m'} \tilde{\phi}_{LM} \tilde{E}_{\ell' m'} \mathcal{W}^{mMm'}_{\ell L \ell'}$$

weight function (geometrical terms)

- real-space based method
  - developped for the Planck 2015 lensing B-mode map paper
  - mask treatment: inpainting of T and apodization
  - based on the Planck 2013 lensing METIS extraction method applied to full-mission data

$$\left(\hat{Q}^{\rm lens} \pm i\hat{U}^{\rm lens}\right) = \mathcal{B}^{-1} \nabla \left(\tilde{Q}^E \pm i\tilde{U}^E\right) \cdot \nabla \tilde{\phi}$$

Filtered version of pure E-mode Q, U maps

filtered lensing potential map

- filters are optimised to minimise the map variance
- $\mathcal{B}^{-1}$, the analytical filtering transfer function ensures the estimator is unbiased

…that give equivalent results

The lensing-B map

PRELIMINARY

$$\tilde{B}^{\rm lens} = \sum_{\ell m} \mathcal{F}_\ell \hat{B}^{\rm lens}_{\ell m} Y_{\ell m}$$ using 2 different filters

Full-resolution Wiener-filtered B-lensing,
nside=2048, FWHM=10 arcmin

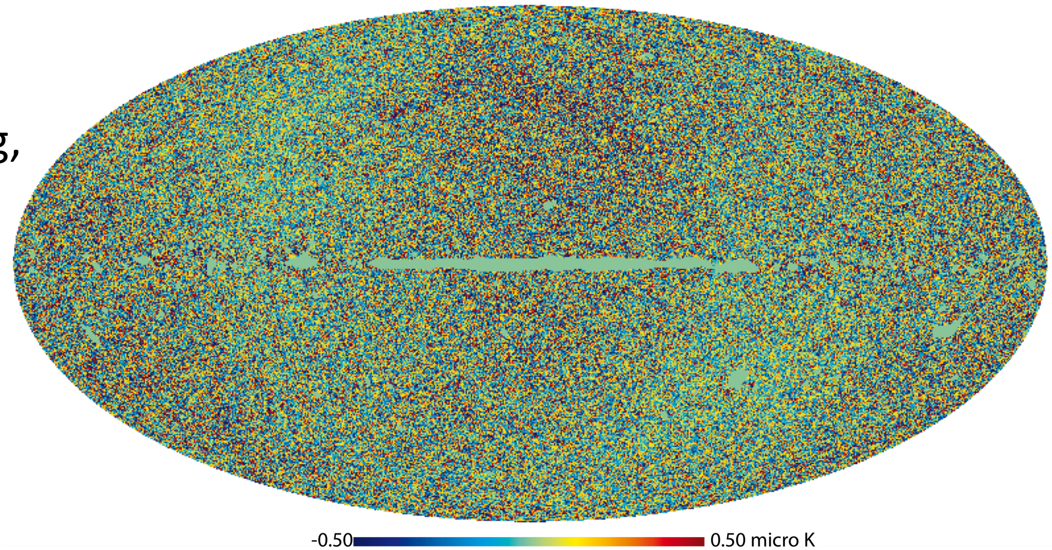

Large scales Wiener-filtered B-lensing,
nside=256, FWHM=60 arcmin

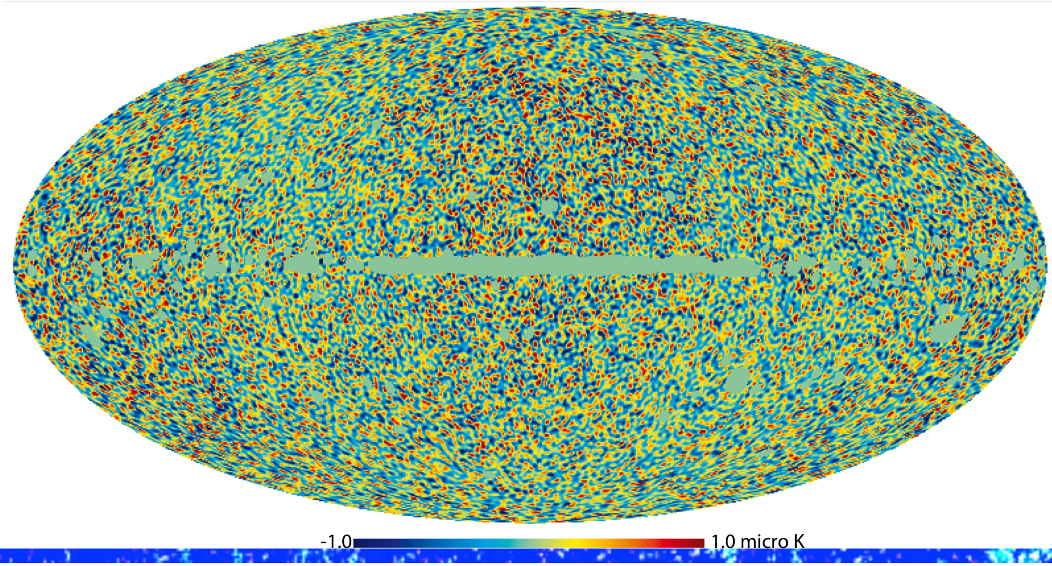

Lensing B power spectrum measurements

Results using different mass tracers:

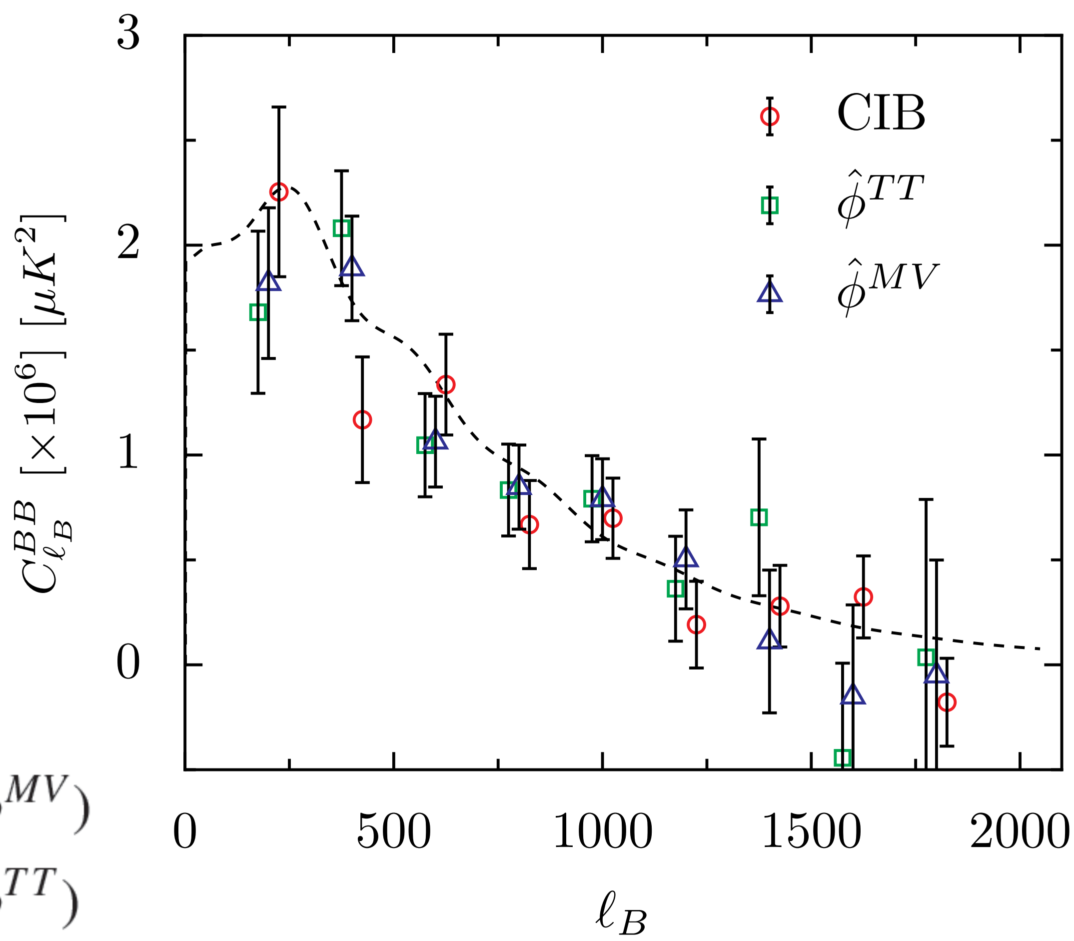

$$\hat{A}^B_{8\to 2048} = 0.93 \pm 0.08 \quad (\phi^{MV})$$
$$\hat{A}^B_{8\to 2048} = 0.95 \pm 0.09 \quad (\phi^{TT})$$
$$\hat{A}^B_{8\to 2048} = 0.93 \pm 0.10 \quad (\text{CIB})$$

→ $\gtrsim 10\sigma$ detection of the lensing-B

Foreground residuals robustness tests

PRELIMINARY

Using foreground-cleaned T, Q, U from different component separation methods [Ref: Planck results XI 2015] with a common $f_{\rm sky} \simeq 70\%$ mask

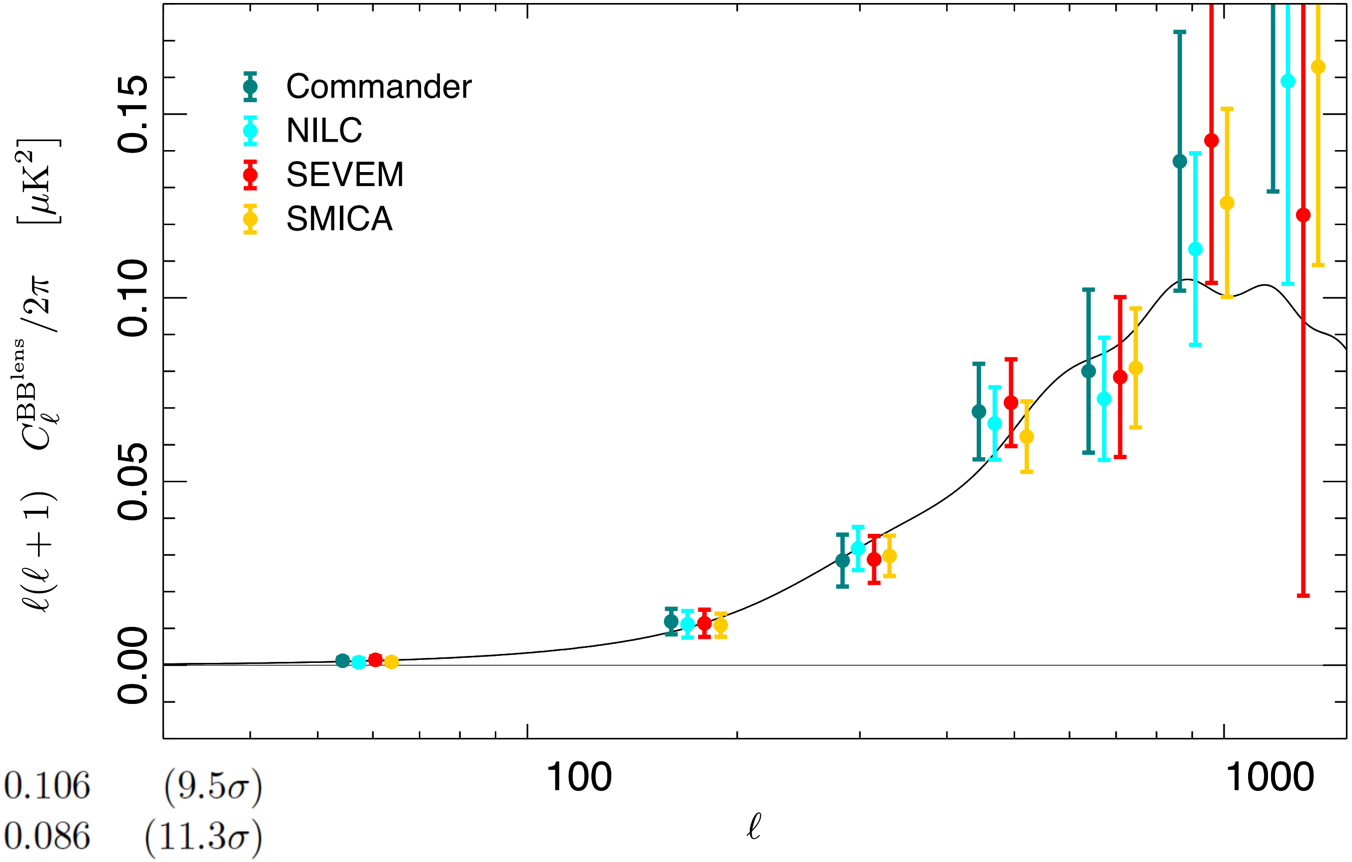

$A_B^{\rm Commander} = 1.007 \pm 0.106 \quad (9.5\sigma)$

$A_B^{\rm NILC} = 0.974 \pm 0.086 \quad (11.3\sigma)$

$A_B^{\rm SEVEM} = 1.000 \pm 0.103 \quad (9.7\sigma)$

$A_B^{\rm SMICA} = 0.970 \pm 0.082 \quad (11.8\sigma)$

→ consistent results based on independant component separations

→ the B-lensing extimate is immune to foreground residuals

Comparison to external measurements

PRELIMINARY

- direct B-mode measurements (i. e. auto-Cl of the observed B-mode)

POLARBEAR 2014
[Ref P.A.R. Ade et al. 2014 (arXiv:1403.2369)]
see Satoru Takakura's talk

BICEP2/Keck 2015
[Ref P.A.R. Ade et al. 2014 (arXiv:1502.00643)]
see Kirit Karkare's talk

- Cross-correlation measurements

SPT 2013
[Ref D. Hanson et al. 2013 (arXiv:1307.5830)]
SPTpol@150GHz + Herschel CIB

see also POLARBEAR 2014
[Ref P.A.R. Ade et al. 2014b (arXiv:1312.6646)]

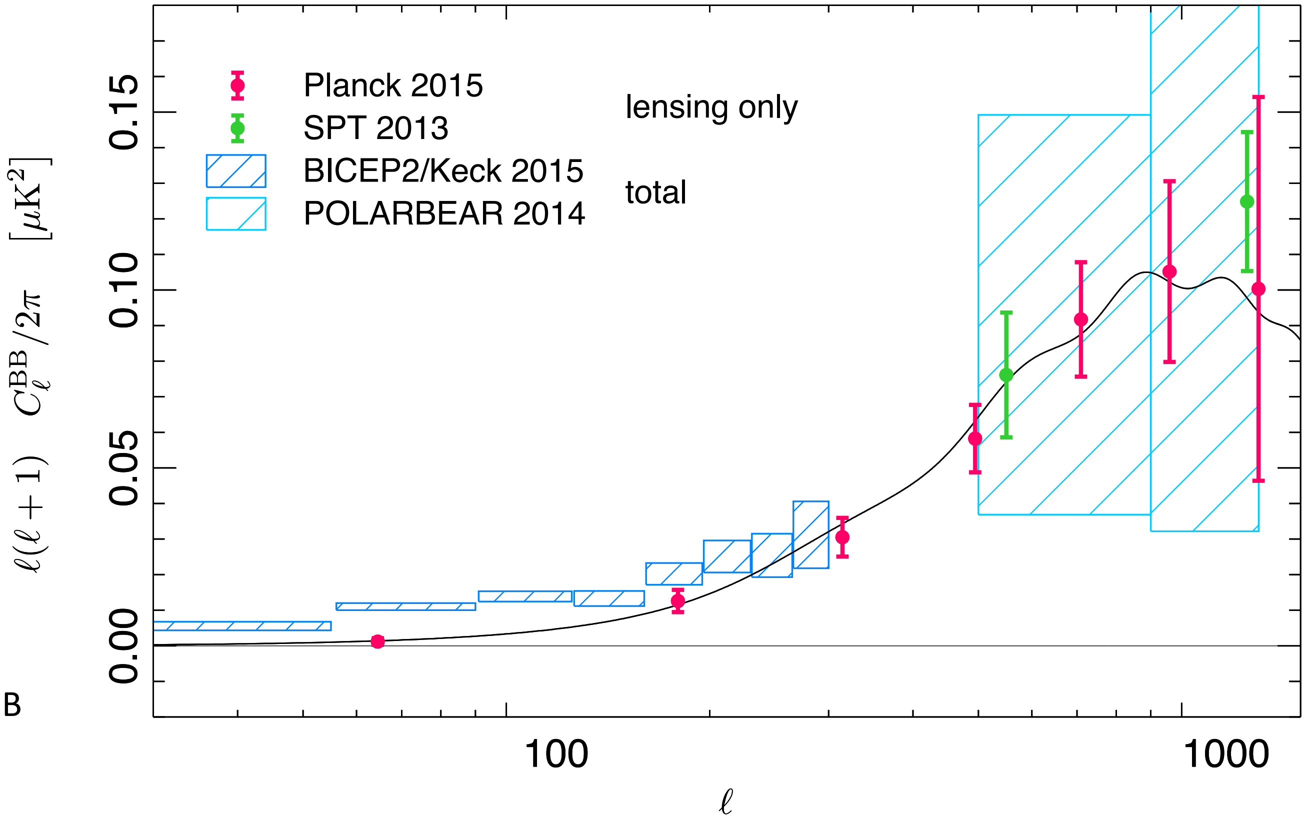

→ no bias at multipole relevant for primordial B-mode search

→ the most accurate B-lensing measurement to date up to $\ell \lesssim 1000$

What is the lensing B map useful for ?

PRELIMINARY

- Measuring the lensing B at the largest angular scales

better than rebuilding a template using ϕ^{MV}

Bicep2/Keck : $\Delta A_{\mathrm{Blens}} = 0.15$

$A_{\mathrm{lens}} = 1.13 \pm 0.18$ [BKP analysis]

POLARBEAR
SPTpol } lensing B at 100<ell<300

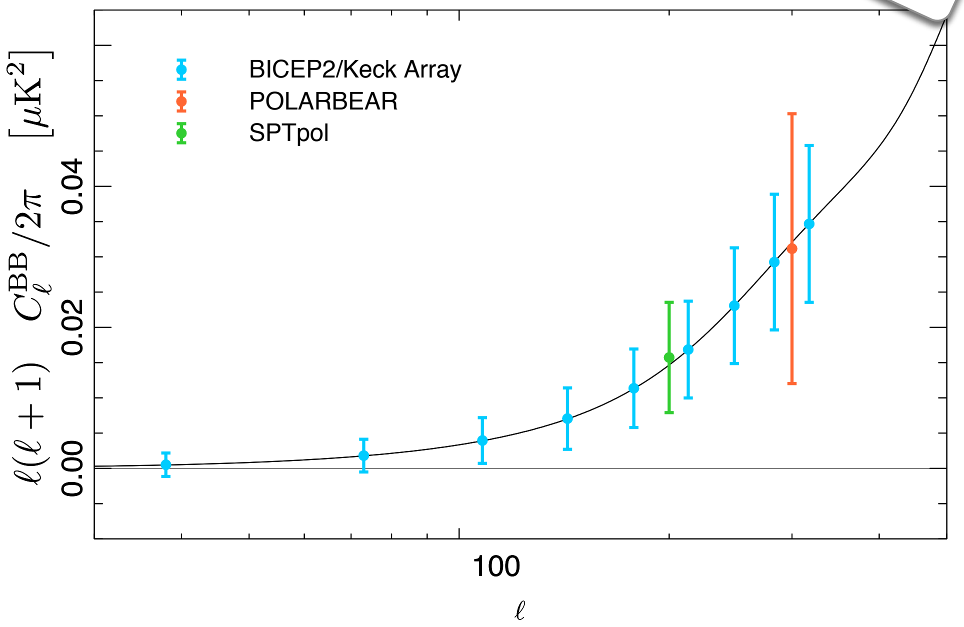

- r, A_lens improvement forecasts

Fisher matrix forecasts in a {LCDM+r+A_lens+A_dust} model

uncertainty reduction	BK [Ade++ 2015]	LiteBIRD [Matsumura++ 2014] [see M. Hazumi's talk]
$\delta(\Delta A_{\mathrm{lens}})$	36 % (ΔA_{lens} = 0.12)	20% (ΔA_{lens} = 0.03)
$\delta(\Delta r)$	5% (Δr = 0.03)	15% (Δr = 1.8x 10-3)

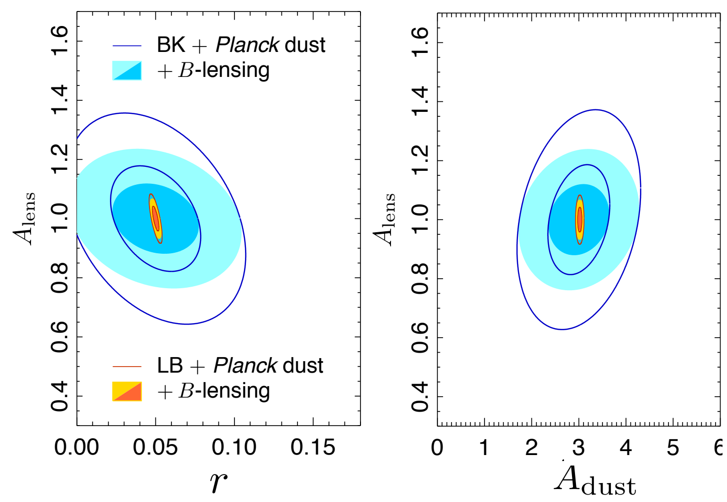

Conclusions

Planck has measured the first nearly full-sky map of the integrated mass distribution (thanks to its observational performancies + high systematic control in the data-processing)

- S/N ≈ 1 at large angular scales (35% uncertainties improvement over the 2013 results)
- valuable dark matter tracer for corss-correlation studies: e.g. first detection of the CIB-Lensing (46s) and ISW-lensing

The lensing power spectrum is measured at 2.5% precision level (best measurement to date)

- passes an extensive suites of cross-checks and robustness tests
- our cleanest multipole range is 40-400 (retains 90% of the S/N)

Several important cosmological impacts (probing the post-recombination history with CMB alone)

- alternative τ measurement (independently of the polarization)
- imposing flatness at the sub-percent level
- weaker constraining power on the extension to LCDM than expected (e.g. low-ell dip tensions)
- mild precision improvement yet important accuracy improvement

First nearly all-sky map of the lensing induced B-modes

- Planck ϕ as mass tracer: including all the lensing information
- >10σ measurement of the lensing B power spectrum (indirect method)
- useful tool for other experiments : measurement of the lensing B at the lowest accessible ell and (A_lens, r) degeracy breaking.

Lensing results are a stricking success of the whole PLANCK collaboration.

The scientific results that we present today are a product of the Planck Collaboration, including individuals from more than 100 scientific institutes in Europe, the USA and Canada.

Planck is a project of the European Space Agency, with instruments provided by two scientific Consortia funded by ESA member states (in particular the lead countries: France and Italy) with contributions from NASA (USA), and telescope reflectors provided in a collaboration between ESA and a scientific Consortium led and funded by Denmark.


Thank you

Additional material for answering questions

Consistency with alternative method

PRELIMINARY

We use the same setup:

- SMICA T and P maps
- TT-only lensing extraction
- lensing bias estimate using FFP8
- $f_{\rm sky} \simeq 70\%$

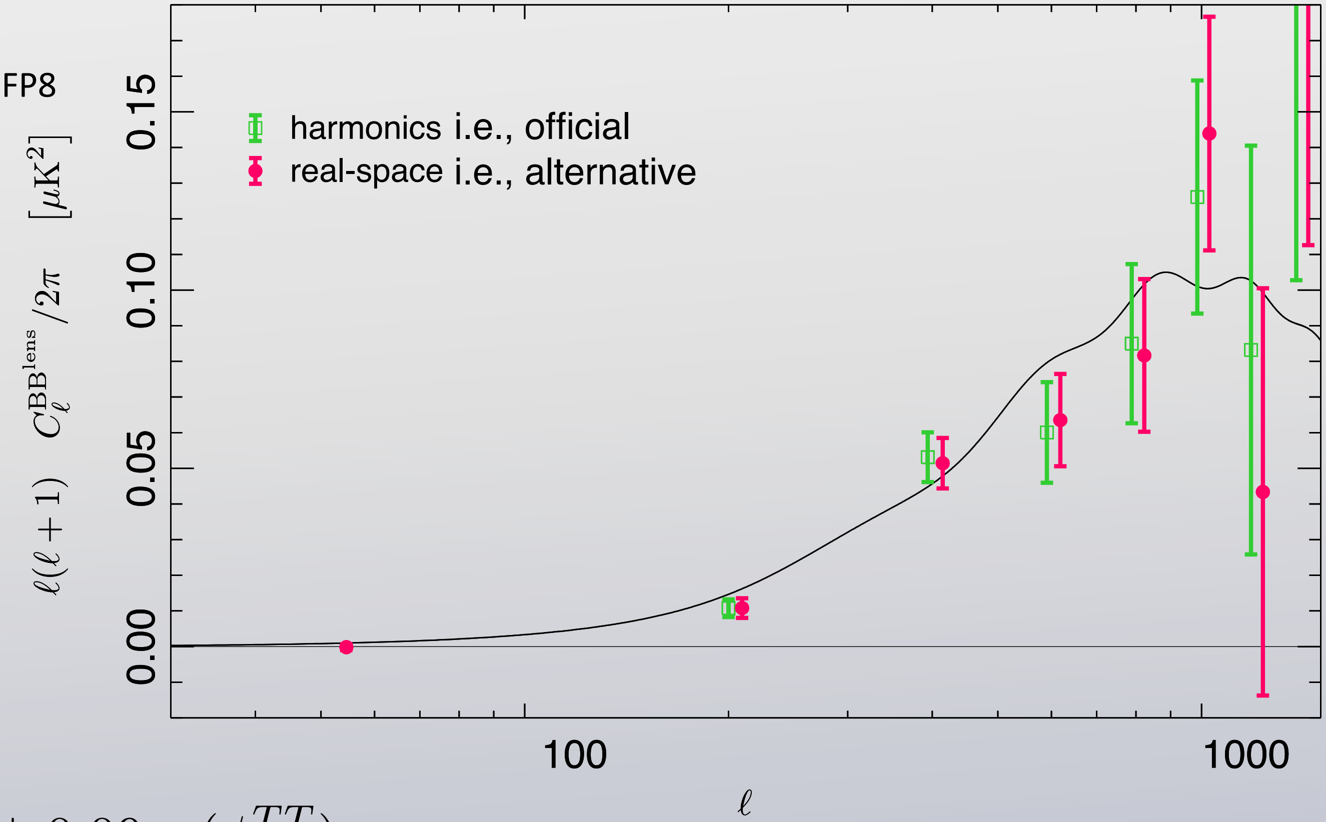

$$\hat{A}_B^{\rm official} = 0.95 \pm 0.09 \quad (\phi^{TT})$$

$$\hat{A}_B^{\rm alternative} = 0.97 \pm 0.08$$

→ consistent results using 2 independent methods

The real-space based alternative pipeline

Further details on the real-space pipeline [Ref: Planck B-lensing paper] :

1. Masking foreground-contaminated areas in the temperature map and inpainting
2. Extracting ϕ using Okamoto&Hu estimator and subtracting for the *Mean-Field*
3. Generating pure E-mode $Q^E \& U^E$ by nullifying the B-mode component in spherical harmonic space
4. Filtering $\phi,\ Q^E \& U^E$ and implementing : $\nabla \left(\tilde{Q}^E \pm i\tilde{U}^E \right) \cdot \nabla \tilde{\phi}$
5. deconvolving from the filtering transfer function

The lensing potential extraction

PRELIMINARY

The consistency of the 2 lensing extraction methods is discussed in Planck 2013 lensing
Quick check on Planck 2014 data:

- the official ϕ of Planck 2014 lensing
  - T+P (25% less uncertainties)
  - minimum-variance filtering of T and P

→ used in the harmonics-space method

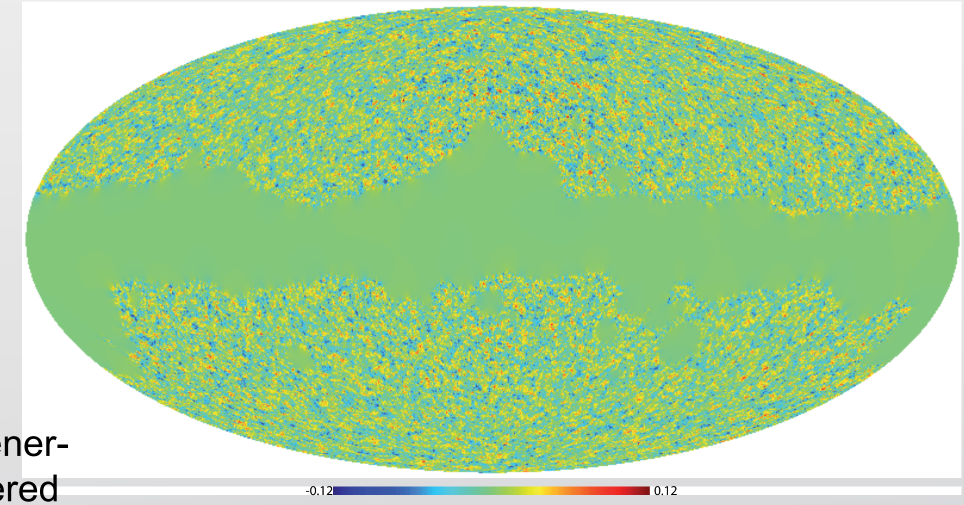

Wiener-filtered convergence maps

- the alternative ϕ :
  - T-only
  - mask treated by inpainting
  - Ref: Planck 2013 lensing

→ targeted to real-space implementation

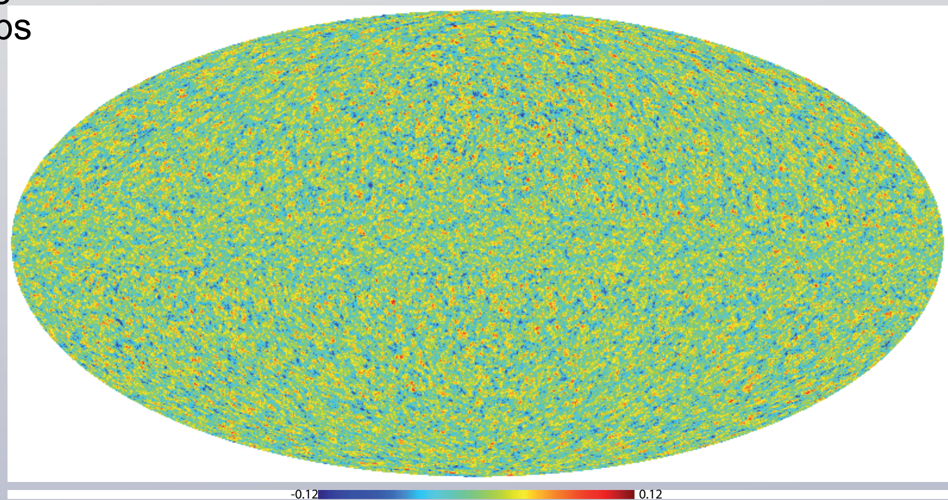

Correlation with other LSS tracers

External data

Planck 2013 Lensing

- 20 sigma correlation with NVSS radio galaxies and quasars (z_{mean} = 1.1)
- 10 sigma with SDSS Luminous Red Galaxies (z_{mean} = 0.55)
- 7 sigma with the WISE satellite IR galaxies catalog (z_{mean} = 0.1)

Planck's Cosmic Infrared Background (CIB)

- unresolved high-redshift dusty star-forming galaxies
- dominant extra-galactic emission at $\geq$ 353GHz

- first detection (42 sigma) of a correlation between high-frequency maps and lensing

stacking: 20 000 T hot spots 20 000 T cold spots random locations

545 GHz

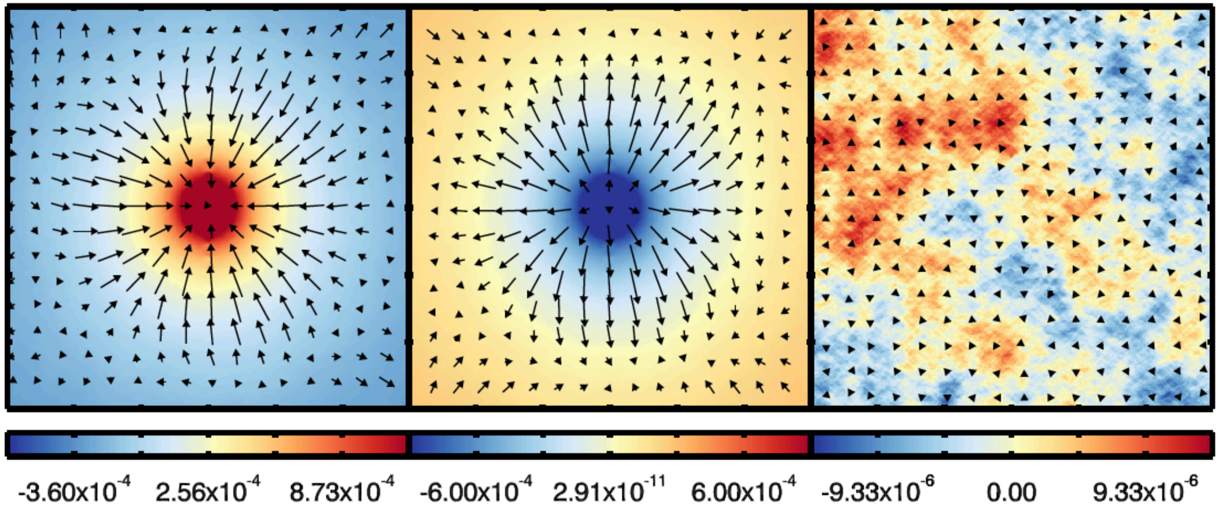

1°

- helps in probing the origin of the CIB hence in constraining the star formation history